



Does the combination of optimal substitutions at the C²-, N⁵- and N⁸-positions of the pyrazolo-triazolo-pyrimidine scaffold guarantee selective modulation of the human A₃ adenosine receptors?

Siew Lee Cheong^{a,†}, Anton V. Dolzhenko^{a,†}, Silvia Paoletta^b, Evelyn Pei Rong Lee^a, Sonja Kachler^c, Stephanie Federico^d, Karl-Norbert Klotz^c, Anna V. Dolzhenko^a, Giampiero Spalluto^{d,*}, Stefano Moro^{b,*}, Giorgia Pastorin^{a,*}

^a Department of Pharmacy, National University of Singapore, 3 Science Drive 2, Block S15, #05-PI-03, 117543 Singapore, Singapore

^b Molecular Modeling Section (MMS), Dipartimento di Scienze Farmaceutiche, Università di Padova, via Marzolo 5, I-35131 Padova, Italy

^c Institut für Pharmakologie, Universität of Würzburg, Versbacher Straße 9, D-97078 Würzburg, Germany

^d Dipartimento di Scienze Chimiche e Farmaceutiche, Università degli Studi di Trieste, Piazzale Europa 1, I-34127 Trieste, Italy

ARTICLE INFO

Article history:

Received 12 June 2011

Revised 10 August 2011

Accepted 11 August 2011

Available online 23 August 2011

Keywords:

2-Phenyl-pyrazolo-triazolo-pyrimidines
Human A₃ adenosine receptor antagonists
Structure–affinity relationship
Affinity
Selectivity

ABSTRACT

In an attempt to study the optimal combination of a phenyl ring at the C²-position and different substituents at the N⁵- and N⁸-positions towards the selective modulation of human A₃ adenosine receptors (hA₃AR), we synthesized a new series of 2-*para*-(un)substituted-phenyl-pyrazolo-triazolo-pyrimidines bearing either a methyl or phenylethyl at N⁸ and chains of variable length at N⁵. Through biological evaluation, it was found that the majority of the compounds had good affinities towards the hA₃AR in the low nanomolar range. Compound **16** possessed the best hA₃AR affinity and selectivity profile (K_ihA₃ = 1.33 nM; hA₁/hA₃ = 4880; hA_{2A}/hA₃ = 1100) in the present series of 2-(substituted)phenyl-pyrazolo-triazolo-pyrimidine derivatives. In addition to pharmacological characterization, a molecular modeling investigation on these compounds further elucidated the effect of different substituents at the pyrazolo-triazolo-pyrimidine scaffold on affinity and selectivity to hA₃AR.

© 2011 Elsevier Ltd. All rights reserved.

1. Introduction

Among the four human adenosine receptor subtypes (A₁, A_{2A}, A_{2B}, A₃), human A₃ adenosine receptor (hA₃AR) is the least characterized.¹ Biochemically, it is coupled to G_i-protein in the cellular membrane, which leads to inhibition of activity of a second mes-

Abbreviations: APCI, atmospheric pressure chemical ionization; ATP, adenosine triphosphate; cAMP, cyclic adenosine monophosphate; CHO cells, Chinese hamster ovary cells; DIPEA, diisopropylethylamine; EL, extracellular loop; EGTA, ethylene glycol tetraacetic acid; G_i, inhibitory G protein; hA₁/A_{2A}/A_{2B}/A₃AR, human A₁/A_{2A}/A_{2B}/A₃ adenosine receptor; [³H]-CCPA, [³H]-2-chloro-6-cyclopentyl adenosine; [³H]-NECA, [³H]-N-ethylcarboxamido adenosine; HPLC, high performance liquid chromatography; MOE, molecular operating environment software; PTP, pyrazolo-triazolo-pyrimidine; rmsd, root mean square deviation; R-PIA, R-N⁶-phenylisopropyladenosine; SAR, structure–affinity relationship; TM, transmembrane; TLC, thin-layer chromatography.

* Corresponding authors. Tel.: +39 040 558 3726; fax: +39 040 52572 (G.S.); tel.: +39 049 8275704; fax: +39 049 8275366 (S.M.); tel.: +65 6516 1876; fax: +65 6779 1554 (G.P.).

E-mail addresses: spalluto@univ.trieste.it (G. Spalluto), stefano.moro@unipd.it (S. Moro), phapg@nus.edu.sg (G. Pastorin).

[†] These authors contributed equally to the manuscript.

senger, adenylyl cyclase, with a subsequent decrease in cyclic adenosine monophosphate (cAMP) levels; other signaling transduction pathways are also reported for this receptor subtype.² Many studies have been performed to identify its pharmacological roles in our body, showing that the modulation of hA₃AR is associated with a number of pathophysiological conditions. Explicitly, the inhibition of the hA₃AR is implicated in the treatment of several diseases, such as glaucoma, asthma and cancer.^{3,4} In light of the biological importance of such receptor, diverse classes of polyheterocyclic scaffolds have been designed and discovered as potential hA₃AR antagonists to-date.^{5,6}

Among these derivatives, the pyrazolo-triazolo-pyrimidines (PTPs) have been identified as highly potent and moderately selective hA₃AR antagonists.^{7–9} From our previous studies, we showed that, among the N⁵-unsubstituted PTPs, the presence of a small group at the N⁸-position was crucial for selective binding to hA₃AR.⁸ Concurrently, the introduction of an amide group, particularly an arylcarbonyl chain at the N⁵-position further improved hA₃AR affinity.¹⁰ In a recent study, we also reported that the new series of PTPs, bearing a phenyl group in place of the C²-furyl ring, not only conferred a good pharmacological profile, but also

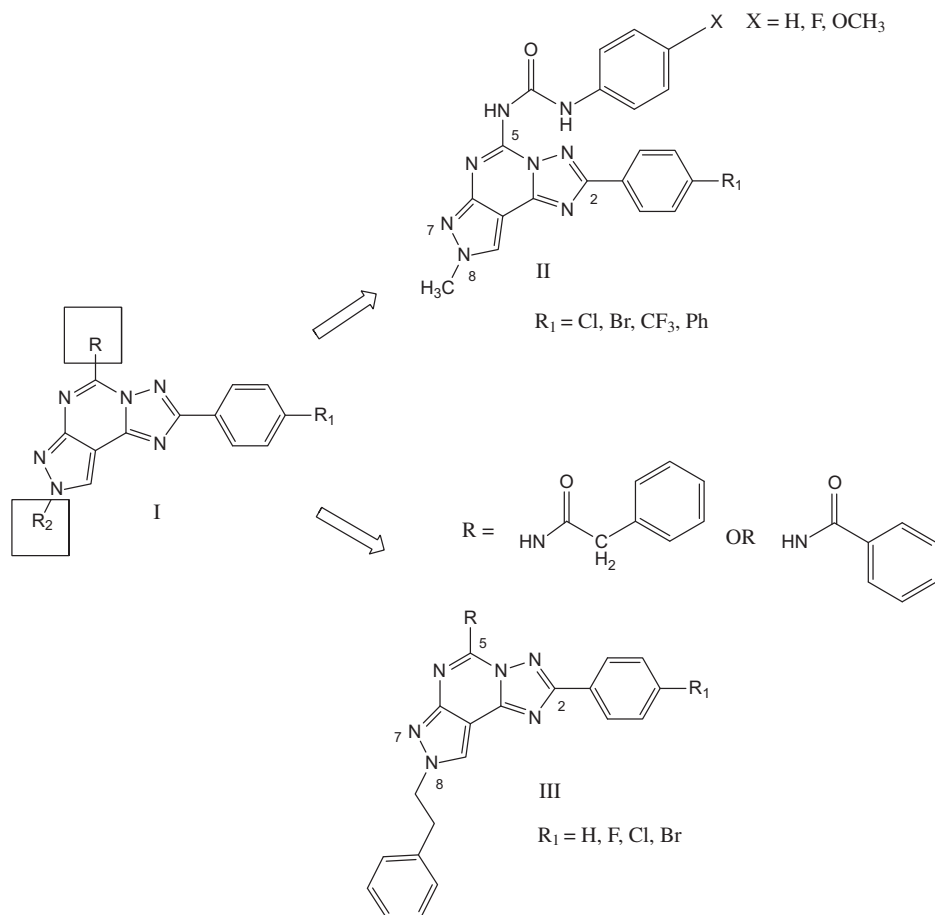


Chart 1. Rational design of new 2-(substituted)phenyl PTPs.

overcame the metabolic transformation of the furan ring into toxic intermediates¹¹ (**I** in Chart 1 and compounds **1–3**, **6**, **7**, **20–25** and **28** in Table 1).

Based on these observations, in this study we thus hypothesized that the combination of a (substituted)phenyl group at the C²-position, together with substituents at the N⁵- and the N⁸-positions deemed optimal for interaction with the hA₃AR, would effectively give rise to new potent and selective A₃AR antagonists. In order to test our hypothesis, a new series of 2-(substituted)phenyl-pyrazolo-triazolo-pyrimidines bearing either a methyl (**II**) or a phenylethyl group (**III**) at the N⁸-position, in conjunction with arylcarbamide, phenylacetamide or benzamide chains at the N⁵-position (Chart 1) was designed and synthesized in the present study. This new series of compounds (compounds **4**, **5**, **8–19**, **26**, **27** and **29–33**) was aimed at further exploring the effect of these substituents at each position of the PTP tricyclic scaffold towards hA₃AR affinity and selectivity. Moreover, to better clarify the effect of these substituents on the binding modes of the new compounds at the hA₃AR, a molecular modeling investigation was also performed.

2. Chemistry

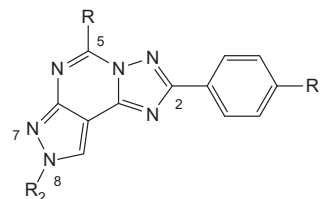
Synthesis of new N⁸-methyl derivatives **4**, **5** and **8–19** was performed using a combination of new steps as well as known procedures (Scheme 1). In order to obtain a methyl group at the N⁸-position of the PTP scaffold in the substituted areas, the preparation of intermediate **38** is a critical step. Several methods have been reported thus far, but all with their limitations.^{12,13} Therefore, a regioselective synthetic procedure that allowed the preparation

of 4-cyano-1-methyl-pyrazol-3-ylamine **38** via a more practical and chromatographic-free process was preferred. The condensation reaction between hydrazine and benzaldehyde gave the intermediate benzyl hydrazone **35** with the benzyl group serving as a protecting group. Subsequent reaction with ethoxymethylene malononitrile, selective methylation with methyl iodide and deprotection with ring closure provided only 4-cyano-1-methyl-pyrazol-3-ylamine **38** in good yield.

Imidate **39** was prepared from 4-cyano-1-methyl-pyrazolo-3-ylamine **38** and triethyl orthoformate using a known procedure.¹² A novel method that has been recently reported by our group¹⁴ was employed for the synthesis of **40**, in which imidate **39** was reacted with hydrazine in ethanol to isolate pure **40**. In the previous study, intermediates **41** and **42** (with R₁ = Cl or Br) were prepared by cyclocondensation of hydrazides with imidate **39**.¹² This method required harsh conditions (260 °C) and chromatographic purification of the products. The poor solubility of **41–44**, particularly when C²-moiety is a substituted phenyl group, made chromatographic purification a time- and solvent-consuming process. Hence, we adopted a more practical process¹⁴ with mild reaction conditions, as shown in steps vi and vii in Scheme 1, to obtain reasonable yields and good purity of intermediates **41–44**.

Subsequent steps were performed using established procedures.^{9,15,16} Treatment of **41–44** with hydrochloric acid at reflux temperature induced pyrimidine ring opening to furnish the 1-methyl-4-(3(5)-aryl-1,2,4-triazol-5(3)-yl)-pyrazol-3-ylamines **45–48** in good yield. These derivatives **45–48** were converted to 2-(substituted)phenyl-8-methyl-pyrazolo[4,3-*e*][1,2,4]triazolo[1,5-*c*]pyrimidin-5-yl amines **2–5** by cyclocondensation with an excess of cyanamide in 1-methyl-2-pyrrolidone at 160 °C.¹²

Table 1
Binding affinity (K_i) at hA₁AR, hA_{2A}AR, hA_{2B}AR and hA₃AR and selectivity against hA₁AR and hA_{2A}AR



Compd	R	R ₁	R ₂	K_i , nM (95% CI)				Selectivity	
				hA ₁ ^a	hA _{2A} ^b	hA _{2B} ^c	hA ₃ ^d	hA ₁ /hA ₃	hA _{2A} /hA ₃
1 ^e	NH ₂	H	N ⁸ -CH ₃	339 (319–359)	121 (100–147)	>10,000	75.0 (63.1–90.4)	4.52	1.61
2 ^e	NH ₂	Cl	N ⁸ -CH ₃	4860 (3360–7010)	2020 (1060–3840)	>10,000	72.4 (71.3–73.6)	67.1	27.9
3 ^e	NH ₂	Br	N ⁸ -CH ₃	2890 (2230–3730)	1500 (1370–1640)	>10,000	38.6 (35.9–41.5)	74.9	38.9
4	NH ₂	CF ₃	N ⁸ -CH ₃	>100,000	6930 (4340–11,100)	>10,000	304 (237–391)	>328.9	22.8
5	NH ₂	Ph	N ⁸ -CH ₃	>100,000	>30,000	>10,000	147 (114–188)	>680	>204
6 ^e	NH-COCH ₂ Ph	Cl	N ⁸ -CH ₃	4850 (3680–6400)	8320 (6180–11,200)	>10,000	0.248 (0.211–0.292)	19,600	33,500
7 ^e	NH-COCH ₂ Ph	Br	N ⁸ -CH ₃	24,400 (13,900–42,900)	>100,000	>10,000	0.345 (0.313–0.381)	70,700	>290,000
8	NH-CO-NH-Ph	Cl	N ⁸ -CH ₃	5550 (4050–7600)	987 (615–1580)	>10,000	1.71 (1.20–2.44)	3250	577
9	NH-CO-NH-Ph	Br	N ⁸ -CH ₃	>10,000	2360 (2160–2570)	>10,000	2.50 (1.89–3.32)	>4000	944
10	NH-CO-NH-Ph	CF ₃	N ⁸ -CH ₃	12,900 (9180–18,200)	36,000 (33,900–38,300)	>10,000	3.44 (2.34–5.05)	3750	10,500
11	NH-CO-NH-Ph	Ph	N ⁸ -CH ₃	>30,000	>30,000	>10,000	5.90 (3.33–10.5)	>5090	>5090
12	NH-CO-NH-(4-F)Ph	Cl	N ⁸ -CH ₃	>30,000	1060 (864–1310)	>10,000	5.30 (4.35–6.45)	>5660	200
13	NH-CO-NH-(4-F)Ph	Br	N ⁸ -CH ₃	>30,000	5930 (3270–10,800)	>10,000	1.72 (0.91–3.26)	>17,400	3450
14	NH-CO-NH-(4-F)Ph	CF ₃	N ⁸ -CH ₃	4420 (1700–11,500)	>30,000	>10,000	1.91 (1.01–3.59)	2310	>15,700
15	NH-CO-NH-(4-F)Ph	Ph	N ⁸ -CH ₃	>100,000	>100,000	>10,000	4.06 (3.17–5.19)	>24,600	>24,600
16	NH-CO-NH-(4-OCH ₃)Ph	Cl	N ⁸ -CH ₃	6490 (3360–12,500)	1460 (1050–2040)	>10,000	1.33 (0.91–1.95)	4880	1100
17	NH-CO-NH-(4-OCH ₃)Ph	Br	N ⁸ -CH ₃	>10,000	8400 (5220–13,500)	>10,000	1.95 (1.64–2.31)	>5130	4310
18	NH-CO-NH-(4-OCH ₃)Ph	CF ₃	N ⁸ -CH ₃	>100,000	>100,000	>10,000	2.36 (1.46–3.80)	>42,400	>42,400
19	NH-CO-NH-(4-OCH ₃)Ph	Ph	N ⁸ -CH ₃	>100,000	>100,000	>10,000	2.10 (1.41–3.14)	>47,600	>47,600
20 ^e	NH ₂	H	N ⁸ -CH ₂ -CH ₂ -Ph	74.8 (51.9–108)	196 (121–317)	>10,000	76.7 (59.5–99.0)	0.975	2.56
21 ^e	NH ₂	F	N ⁸ -CH ₂ -CH ₂ -Ph	39.1 (31.9–47.9)	127 (106–151)	>10,000	50.6 (32.9–78.0)	0.773	2.51
22 ^e	NH ₂	Cl	N ⁸ -CH ₂ -CH ₂ -Ph	204 (159–262)	2180 (1400–3410)	>10,000	79.7 (67.9–93.6)	2.56	27.4
23 ^e	NH ₂	Br	N ⁸ -CH ₂ -CH ₂ -Ph	498 (327–758)	>30,000	>10,000	221 (152–320)	2.25	>136
24 ^e	NH ₂	OCH ₃	N ⁸ -CH ₂ -CH ₂ -Ph	289 (232–359)	1400 (895–2210)	>10,000	25 (17.5–35.6)	11.6	56.0
25 ^e	NH-COPh	H	N ⁸ -CH ₂ -CH ₂ -Ph	313 (209–468)	963 (749–1240)	>10,000	23.9 (20.3–28.1)	13.1	40.3
26	NH-COPh	F	N ⁸ -CH ₂ -CH ₂ -Ph	395 (318–492)	4040 (3500–4620)	>30,000	17.1 (14.9–19.8)	23.1	236
27	NH-COPh	Cl	N ⁸ -CH ₂ -CH ₂ -Ph	221 (196–251)	19,400 (11,900–31,400)	>30,000	11.4 (9.94–13.0)	19.4	1700
28 ^e	NH-COPh	Br	N ⁸ -CH ₂ -CH ₂ -Ph	270 (191–382)	>100,000	>10,000	153 (120–195)	1.76	>654
29	NH-COPh	OCH ₃	N ⁸ -CH ₂ -CH ₂ -Ph	831 (530–1300)	25,200 (22,300–28,400)	>10,000	28.9 (22.0–37.9)	28.8	872
30	NH-COCH ₂ Ph	H	N ⁸ -CH ₂ -CH ₂ -Ph	192 (167–220)	614 (574–656)	>30,000	3.02 (1.49–6.11)	63.6	203
31	NH-COCH ₂ Ph	F	N ⁸ -CH ₂ -CH ₂ -Ph	232 (209–259)	571 (507–642)	>30,000	3.34 (3.16–3.53)	69.5	171
32	NH-COCH ₂ Ph	Cl	N ⁸ -CH ₂ -CH ₂ -Ph	932 (688–1260)	3090 (2680–3560)	>30,000	8.48 (4.81–14.9)	110	364
33	NH-COCH ₂ Ph	Br	N ⁸ -CH ₂ -CH ₂ -Ph	>10,000	>10,000	>10,000	>10,000	NA	NA

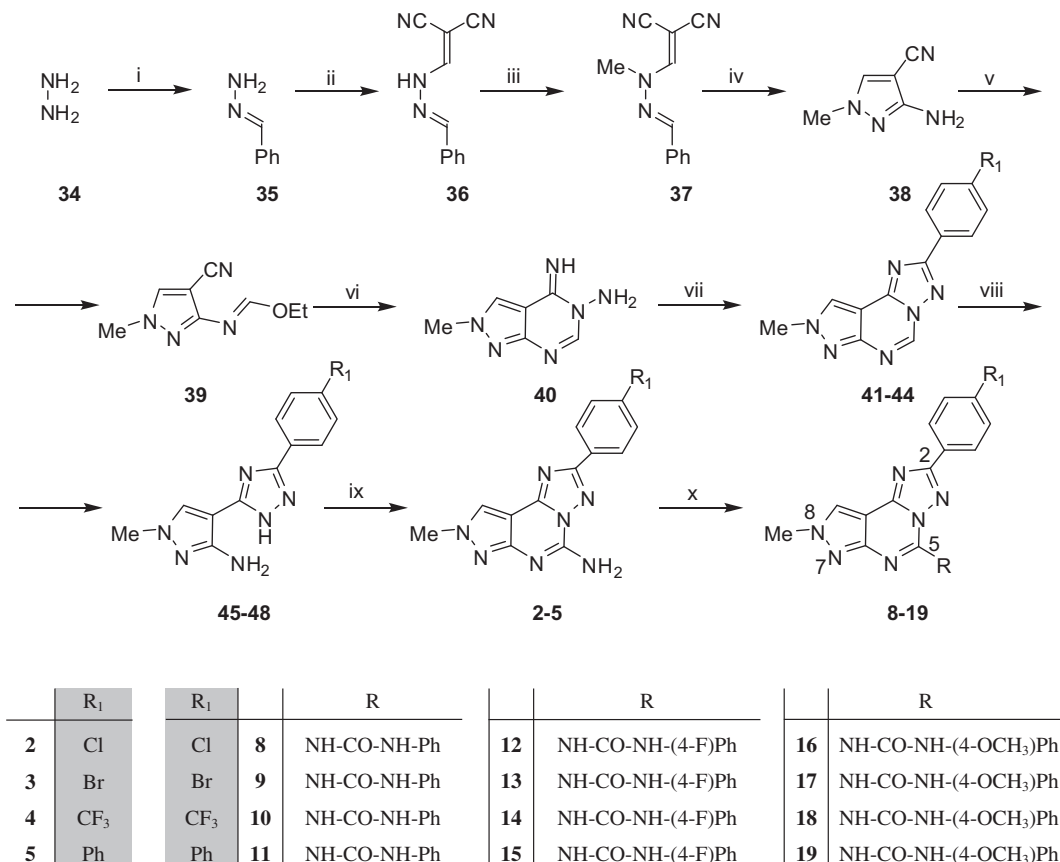
^a Displacement of specific [³H]-CCPA binding at hA₁AR expressed in CHO cells, ($n = 3–6$).

^b Displacement of specific [³H]-NECA binding at hA_{2A}AR expressed in CHO cells, ($n = 3–6$).

^c K_i values of the inhibition of NECA-stimulated adenylyl cyclase activity in CHO cells, ($n = 3–6$).

^d Displacement of specific [³H]-NECA binding at hA₃AR expressed in CHO cells, ($n = 3–6$). Data are expressed as geometric means, with 95% confidence limits.

^e Data taken from Ref. 11.



Scheme 1. Synthetic schemes for compounds **2–5** and **8–19**. Reagents: (i) PhCHO; (ii) (NC)₂C=CH(OEt); (iii) MeI, NaOH; (iv) conc. HCl, reflux; (v) HC(OEt)₃; (vi) H₂NNH₂; (vii) (1) R₁CHO, Et₃N, (2) PhI(OAc)₂; (viii) HCl, reflux; (ix) H₂NCN, TsOH; (x) R₂N=C=O.

Substituted ureas **8–19** were obtained by reaction of the substituted amines **2–5** with the appropriate isocyanate in toluene under reflux.

The synthetic pathways for the new series of 5-amide-8-phenylethyl-2-(*para*-(un)substituted)phenyl-pyrazolo-[4,3-*e*]1,2,4-triazolo[1,5-*c*]pyrimidine derivatives **26**, **27** and **29–33** were based on known procedures as described in Refs. 11,17,18 (Scheme 2).^{11,17,18} The inseparable mixtures of N¹ and N² regioisomers for alkylated 3(5)-amino-4-cyano-pyrazoles (**50** and **51**) were synthesized through alkylation reaction between (2-iodoethyl)benzene and 3(5)-amino-4-cyano-pyrazole (**49**). These intermediates were directly refluxed in triethyl orthoformate to give the corresponding imidates (**52** and **53**), and they were subsequently reacted with the appropriate (*para*-substituted)benzoic hydrazides in refluxing 2-methoxy-ethanol to afford the intermediates **54–58**. Next, these compounds were subjected to a thermally induced cyclization in diphenyl ether at about 260 °C. After the chromatographic separation of N⁷ (minor product) and N⁸ (major product) regioisomers, they provided the tricyclic compounds (**59–63**) in rather good yield (about 60% for N⁸ derivatives and 30% for N⁷ derivatives). Hydrolysis in 20% HCl gave rise to the corresponding aminotriazoles (**64–68**), which were subsequently converted into the 5-amino-8-phenylethyl-2-(*para*-substituted)phenylpyrazolo-[4,3-*e*]1,2,4-triazolo[1,5-*c*]pyrimidine derivatives (**20–24**).

Some of these 2-(substituted)phenyl-pyrazolo-[4,3-*e*]1,2,4-triazolo[1,5-*c*]pyrimidin-5-amines were dispersed in toluene and treated with either benzoic anhydride or phenylacetyl chloride (Scheme 3). The mixture was heated under reflux and stirred for 12–24 h. The solvent was later removed under reduced pressure

and the residue was subjected to chromatographic purification, to afford the desired compounds (**26**, **27** and **29–33**).

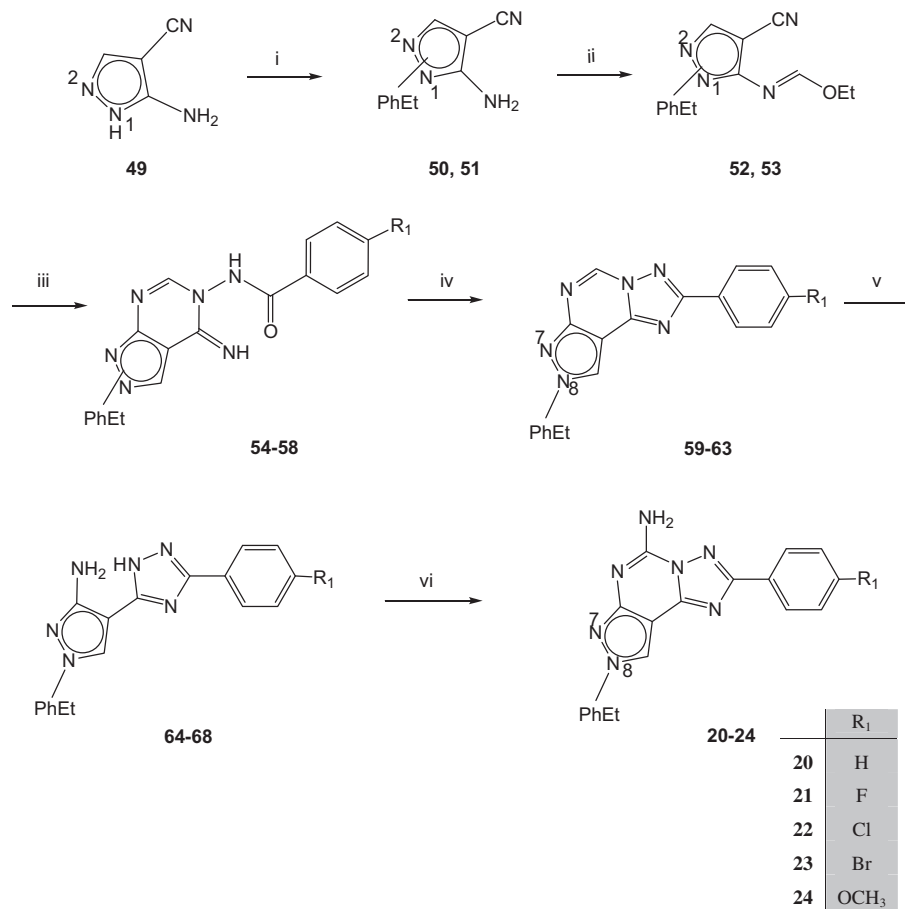
3. Biology

3.1. Binding assay at hA₁, hA_{2A}, and hA₃ ARs

The affinity of an antagonist towards its receptor (expressed in Chinese Hamster Ovary cells (CHO) for hA₁, hA_{2A}, hA₃ AR) was evaluated through the measurement of displacement of selective radioligands,^{11,19–22} which were previously bound to the receptor expressed at the cell surface. In this assay, the displacement was evaluated of: (i) specific [³H]CCPA binding at the hA₁AR; and (ii) specific [³H]NECA binding at both the hA_{2A}AR and hA₃AR. The data were expressed as K_i (dissociation constant), which was calculated from the Cheng and Prusoff equation,²² with geometric means of at least three experiments including 95% confidence intervals.

3.2. Adenylyl cyclase activity assay at hA_{2B}AR

Due to the lack of a suitable radioligand for hA_{2B}AR in binding assay, the potency of antagonists on hA_{2B}AR (expressed on CHO cells) was determined in adenylyl cyclase experiments instead.¹¹ The procedure was carried out as described previously in Klotz et al. with minor modifications.^{19,20} In this assay, an adenosine agonist (NECA) at known concentration was subjected to inhibitory effect of tested antagonist. As a consequence, the activation of adenylyl cyclase was inhibited by such tested antagonist with a following decrease of the cAMP level.



Scheme 2. Synthetic schemes for compounds **20–24**. Reagents: (i) NaH, PhCH₂CH₂I, dimethylformamide; (ii) HC(OEt)₃, reflux; (iii) 2-(4-substituted)benzoic hydrazide, MeO(CH₂)₂OH; (iv) Ph₂O, 260 °C, flash chromatography; (v) HCl, reflux; (vi) NH₂CN, 1-methyl-2-pyrrolidone, pTsOH, reflux.

4. Molecular modeling

A receptor-driven molecular modeling investigation has been performed in order to rationalize the results obtained from the pharmacological evaluation. To that purpose, we conducted molecular docking simulations of the new PTP derivatives on the recently published hA₃AR model.^{23,24} As previously described, this hA₃AR model was built based on the template of the hA_{2A}AR crystallographic structure in complex with the high affinity antagonist ZM-241385 (PDB code: 3EML)²⁵ (methodological details were summarized in the Section 7).^{23,24}

In the process of selecting a reliable docking protocol to be employed in the following docking studies of these new derivatives, we have evaluated the ability of different docking softwares in reproducing the crystallographic pose of ZM-241385 inside the binding cavity of hA_{2A}AR. Among the four different types of programs used to calibrate our docking protocol, the Gold programs was finally chosen since it showed the best performance in regards to the calculated root mean square deviation (RMSD) values relative to the crystallographic pose of ZM-241385.²³ Consequently, based on the selected docking protocol, all the newly synthesized phenyl-pyrazolo[4,3-*e*]1,2,4-triazolo-[1,5-*c*]-pyrimidines were docked into the orthosteric transmembranes (TMs) binding cavity of hA₃AR.

Besides that, in order to analyze the possible ligand–receptor recognition mechanism in a more quantitative manner, we also calculated the individual electrostatic and hydrophobic contributions to the interaction energy of each receptor residues involved in the binding interaction with ligands.

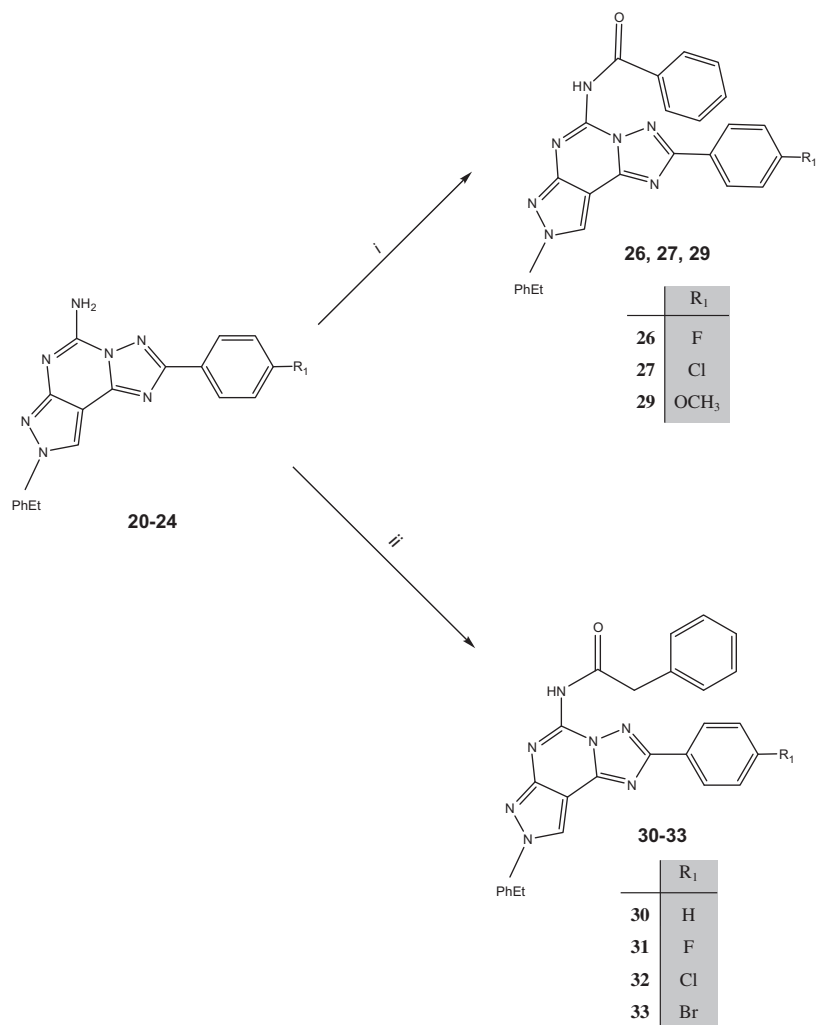
5. Results and discussion

5.1. Structure–affinity relationship studies

A new series of 2-(*para*-(un)substituted)phenyl-pyrazolo[4,3-*e*]1,2,4-triazolo-[1,5-*c*]-pyrimidines was successfully synthesized and characterized. We introduced only a few modifications to the original PTP scaffold, in order to focus our investigation on the combination of optimal substituents at the C²-, N⁵- and N⁸-positions. To that end, we selected a (substituted)phenyl group at the C²-position and either a methyl (compounds **4**, **5** and **8–19**) or a phenylethyl (compounds **26**, **27** and **29–33**) group at N⁸, with concurrent introduction of different amide moieties at position N⁵. Table 1 summarizes the receptor binding affinities of these compounds determined to hA₁AR, hA_{2A}AR and hA₃AR and the corresponding adenylyl cyclase activity in CHO cells that express hA_{2B}AR. The results showed that the new series of 2-(substituted)phenyl-pyrazolo-triazolo-pyrimidines presented good affinity to hA₃AR, as indicated by the nanomolar range of K_i values and, most importantly, improved selectivities over other AR subtypes.

5.1.1. N⁸-Methyl derivatives

From our recent study, it was observed that the bioisosteric replacement of the furan ring at the C²-position with a phenyl ring resulted in a 3- to 8-fold increase in affinity towards hA₃AR and a significant improvement in selectivity (of 2–3 orders of magnitude) over other AR subtypes, namely hA₁AR, hA_{2A}AR and hA_{2B}AR. In other words, compounds with a phenyl ring at the C²-position



Scheme 3. Synthetic schemes for compounds **26**, **27**, **29–33**. Reagents: (i) benzoic anhydride, toluene, reflux; (ii) phenylacetyl chloride, DIPEA, toluene, reflux.

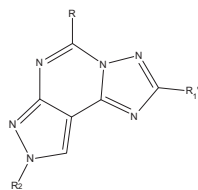
demonstrated better affinity and selectivity profiles towards hA₃AR as compared with the 2-furyl counterparts.¹¹ Nonetheless, in the present investigation we noticed a different trend of hA₃AR affinities in the new series of 2-(*para*-(un)substituted)phenyl-8-methyl-PTPs bearing arylcarbamoyl moieties at the N⁵-position (**4**, **5** and **8–19**), despite the fact that these compounds still maintained good hA₃AR affinity at low nanomolar range (1.3–5.9 nM). It was found that the bioisosteric replacement of the existing furan ring with a phenyl ring in this group of compounds caused 7- to 37-fold decrease in affinity to hA₃AR. Notably, the selectivity over other AR subtypes of these 2-phenyl-PTP derivatives (e.g. compound **10**, with K_ihA₃ = 3.44 nM; hA₁/hA₃ = 3750; hA_{2A}/hA₃ = 10,500 and compound **18**, with K_ihA₃ = 2.36 nM; hA₁/hA₃ >42,400; hA_{2A}/hA₃ >42,400) was still greatly improved in comparison with that of 2-furyl analogues (e.g. compound **70**, with K_ihA₃ = 0.16 nM; hA₁/hA₃ = 3713; hA_{2A}/hA₃ = 2381 and compound **71**, with K_ihA₃ = 0.20 nM; hA₁/hA₃ = 5495; hA_{2A}/hA₃ = 6950) (Table 2). These findings suggested that for this group of N⁸-methyl-PTP-N⁵-arylcarbamides, the 2-furyl ring was more favourable than the 2-phenyl ring for hA₃AR affinity. Even so, the introduction of a phenyl ring at the C²-position was deemed crucial to confer higher selectivity towards hA₃AR in comparison with the 2-furyl ring, while maintaining good affinity at the hA₃AR.

In addition, we also evaluated the effect of *para*-substituents on the 2-phenyl ring towards the affinity profile of hA₃AR. Based on

the binding results, the substituents (e.g. Cl, Br, CF₃, Ph) at the *para*-position of the C²-phenyl ring were found to modulate hA₃AR affinity to a certain extent. The introduction of functional groups with relatively high molecular volume, such as a 4-trifluoromethyl (e.g. compound **4**, with K_ihA₃ = 304 nM) and a 4-phenyl ring (e.g. compound **5**, with K_ihA₃ = 147 nM) on the 2-phenyl ring of some N⁵-unsubstituted derivatives seemed unfavourable for hA₃AR affinity, as shown by their high nanomolar K_i values. From these findings we could infer that the presence of bulky groups at the *para*-position of the C²-phenyl ring was undesirable for the hA₃AR affinity. In contrast, the situation improved remarkably when the same derivatives were further substituted at the N⁵-position. The additional chains at N⁵ (as shown in compounds **10** and **11**) enabled an increase of affinity to hA₃AR with a concomitant decrease of binding to hA₁AR and hA_{2A}AR. This observation implied that the hA₃AR binding cavity around the N⁵-position was spacious enough to accommodate extended chains including the phenylacetyl (compounds **6** and **7**)¹¹ and arylcarbamoyl groups (compounds **8–19**). Among these substituents, the relatively flexible phenylacetyl group (e.g. compound **7**, with K_ihA₃ = 0.345 nM, hA₁/hA₃ = 70,700; hA_{2A}/hA₃ >290,000)¹¹ showed a better binding profile than the arylcarbamoyl chain (e.g. compound **9**, with K_ihA₃ = 2.50 nM, hA₁/hA₃ >4000; hA_{2A}/hA₃ = 944).

Further incorporation of *para*-substituents such as 4-fluoro (compounds **12–15**) and 4-methoxy (compounds **16–19**) groups

Table 2
Binding affinity (K_i) at hA_3AR and selectivity against hA_{1AR} and hA_{2AAR} for compounds **10**, **18**, **20**, **30** (2-*para*-(un)substituted-phenyl-PTPs) and **69–72** (2-furyl-PTPs)



Compd	R	R ₁ '	R ₂	hA_3 (K_i , nM)	hA_1/hA_3	hA_{2A}/hA_3
10	NH-CO-NH-Ph	Ph- <i>p</i> -CF ₃	N ⁸ -CH ₃	3.44	3750	10,500
69	NH-CO-NH-Ph	Furyl	N ⁸ -CH ₃	0.16 ^a	3713 ^a	2381 ^a
18	NH-CO-NH-(4-OCH ₃)Ph	Ph- <i>p</i> -CF ₃	N ⁸ -CH ₃	2.36	>42,400	>42,400
70	NH-CO-NH-(4-OCH ₃)Ph	Furyl	N ⁸ -CH ₃	0.20 ^a	5485 ^a	6950 ^a
20	NH ₂	Ph	N ⁸ -CH ₂ -CH ₂ -Ph	76.7	0.975	2.56
71	NH ₂	Furyl	N ⁸ -CH ₂ -CH ₂ -Ph	300 ^b	0.33 ^b	0.009 ^b
30	NH-CO-CH ₂ -Ph	Ph	N ⁸ -CH ₂ -CH ₂ -Ph	3.02	63.6	203
72	NH-CO-CH ₂ -Ph	Furyl	N ⁸ -CH ₂ -CH ₂ -Ph	45.0 ^c	2.67 ^c	1.33 ^c

^a Data taken from Ref. 10.

^b Data taken from Ref. 17.

^c Data taken from Ref. 26.

on the phenyl ring of arylcarbamoyl moiety seemed tolerable for hA_3AR affinity giving values in the range of 1.33–5.30 nM. Except for derivative **12**, compounds with 4-fluoro and 4-methoxy groups on the phenyl ring of arylcarbamoyl moiety generally possessed better hA_3AR affinities in comparison with the N⁵-phenylcarbamoyl-substituted analogues (e.g. compound **13**, with $K_i hA_3 = 1.72$ nM, $hA_1/hA_3 > 17,400$; $hA_{2A}/hA_3 = 3450$ vs compound **9**, with $K_i hA_3 = 2.50$ nM, $hA_1/hA_3 > 4000$; $hA_{2A}/hA_3 = 944$). Nonetheless, they were still less potent than the N⁵-phenylacetamidic derivatives (e.g. compound **7**, with $K_i hA_3 = 0.345$ nM, $hA_1/hA_3 = 70,700$; $hA_{2A}/hA_3 > 290,000$). Furthermore, the 4-methoxy-phenylcarbamoyl chain at the N⁵-position was shown to confer good selectivity against the hA_{1AR} , hA_{2AAR} and hA_{2BAR} AR as well. In general, there were no substantial differences between the electron-withdrawing (e.g. 4-fluoro in compounds **12–15**) and the electron-donating (e.g. 4-methoxy in compounds **16–19**) effects of such *para*-substituents on hA_3AR affinity, thus implying that the steric effects might be more prominent on the hA_3AR binding profiles of these new PTPs.

5.1.2. N⁸-Phenylethyl derivatives

As reported in our recent study, it was found that when a small alkyl group, like a methyl, was present at the N⁸-position, compounds (**1–19**) showed a preference for hA_3AR , regardless of substitutions at the C²- and N⁵-positions (e.g. compounds **3** [(with a 4-bromophenyl at C² and a free amino at N⁵), $K_i hA_3 = 38.6$ nM; $hA_1/hA_3 = 74.9$; $hA_{2A}/hA_3 = 38.9$] **7** [(with a 4-bromophenyl at C² and a phenylacetamide at N⁵), $K_i hA_3 = 0.345$ nM; $hA_1/hA_3 = 70,700$; $hA_{2A}/hA_3 > 290,000$] and **9** [(with a 4-bromophenyl at C² and a phenylcarbamide at N⁵), $K_i hA_3 = 2.50$ nM; $hA_1/hA_3 > 4000$; $hA_{2A}/hA_3 = 944$]). Conversely, when a longer chain (e.g. phenylethyl group) was introduced at N⁸, we observed a different trend for derivatives bearing a free or substituted amino group at the N⁵-position. When a free amino group was present at the N⁵-position, the presence of an N⁸-phenylethyl group seemed to be responsible for the lower affinities and selectivities of compounds **20–24** for hA_3AR as compared with the N⁸-methyl analogues (e.g. compound **22**, with $K_i hA_3 = 79.7$ nM; $hA_1/hA_3 = 2.56$; $hA_{2A}/hA_3 = 27.4$ vs compound **2**, with $K_i hA_3 = 72.4$ nM; $hA_1/hA_3 = 67.1$; $hA_{2A}/hA_3 = 27.9$). On the other hand, when the same derivatives were further substituted at the N⁵-position, the presence of such additional groups at N⁵ seemed to be always favourable for hA_3AR affinity (e.g. compound **30**, with $K_i hA_3 = 3.02$ nM; $hA_1/hA_3 = 63.6$;

$hA_{2A}/hA_3 = 203$). However, the hA_3AR affinities and selectivities of such N⁸-phenylethyl derivatives were found to be remarkably lower than those of the N⁸-methyl analogues: compound **32**, bearing a N⁵-phenylacetamide, a 4-chlorophenyl at C² and an N⁸-phenylethyl groups showed a 30-fold drop in hA_3AR affinity ($K_i hA_3 = 8.48$ nM; $hA_1/hA_3 = 110$; $hA_{2A}/hA_3 = 364$) in comparison with the N⁸-methyl analogue (compound **6**, with $K_i hA_3 = 0.248$ nM; $hA_1/hA_3 = 19,600$; $hA_{2A}/hA_3 = 33,500$). This might be due to the reason that in the N⁵-unsubstituted derivatives, there was still enough space for the bulky phenylethyl group to orient itself inside the hA_3AR binding cavity. Once an additional group was introduced at the N⁵-position, there was limited space remaining to anchor the phenylethyl, thus causing a considerable decrease in hA_3AR affinity. Between the two N⁵-phenylacetyl and N⁵-benzoyl moieties, the relatively flexible phenylacetyl group (e.g. compounds **31**, with $K_i hA_3 = 3.34$ nM; $hA_1/hA_3 = 69.5$; $hA_{2A}/hA_3 = 171$ and **32**, with $K_i hA_3 = 8.48$ nM; $hA_1/hA_3 = 110$; $hA_{2A}/hA_3 = 364$) showed relatively better binding profiles than those with the shorter benzoyl chain (e.g. compounds **26**, with $K_i hA_3 = 17.1$ nM; $hA_1/hA_3 = 23.1$; $hA_{2A}/hA_3 = 236$ and **27**, with $K_i hA_3 = 11.4$ nM; $hA_1/hA_3 = 19.4$; $hA_{2A}/hA_3 = 1700$). Such observations were consistent with the findings obtained for the N⁸-methyl series of 2-phenyl-PTP derivatives reported previously.¹⁴

We also investigated the impact of 2-furyl ring substitution with a 2-phenyl ring in the current N⁸-phenylethyl series of 2-phenyl-PTPs towards hA_3AR affinities and selectivities. The binding assays results were compared between the new 2-(substituted)phenyl derivatives (e.g. compounds **20** and **30**) and the 2-furyl counterparts (e.g. compounds **72** and **73**)^{17,26} (Table 2). It was observed that the bioisosteric replacement of existing furan ring with a phenyl ring resulted in about 4- to 15-fold increase in affinity towards hA_3AR and considerable improvements in selectivity (of 2- to 3 orders of magnitude) over the other AR subtypes. Such compounds with a phenyl ring at C² and a phenylethyl group at N⁸ showed better affinity and selectivity profiles towards the hA_3AR in comparison with their 2-furyl counterparts, and this further strengthened our previous finding that the substituted-phenyl at the C²-position indeed played a crucial role on the hA_3AR affinity and selectivity against other ARs.

In particular, among the substituents introduced at the *para*-position of the C²-phenyl ring, both the fluoro and chloro groups exerted more favourable effects on hA_3AR affinity in the N⁵-benzamide-substituted (e.g. compound **26**, with $K_i hA_3 = 17.1$ nM;

$hA_1/hA_3 = 23.1$; $hA_{2A}/hA_3 = 236$) and N^5 -phenylacetamide-substituted (e.g. compound **31**, with $K_i hA_3 = 3.34$ nM; $hA_1/hA_3 = 69.5$; $hA_{2A}/hA_3 = 171$) derivatives. Moreover, the presence of two *para*-substituents on the 2-phenyl ring was shown to confer good selectivity against hA_1AR , $hA_{2A}AR$ and $hA_{2B}AR$. Although all the compounds with a 4-bromo group in the N^8 -methyl series showed good affinities at hA_3AR (e.g. compound **3**, with $K_i hA_3 = 38.6$ nM; $hA_1/hA_3 = 74.9$; $hA_{2A}/hA_3 = 38.9$ nM; and compound **7**, with $K_i hA_3 = 0.345$ nM; $hA_1/hA_3 = 70,700$; $hA_{2A}/hA_3 > 290,000$), its pres-

ence in the N^8 -phenylethyl-substituted derivatives (e.g. compound **23**, with $K_i hA_3 = 221$ nM; $hA_1/hA_3 = 2.25$; $hA_{2A}/hA_3 > 136$; and compound **33**, with $K_i hA_3 > 10,000$ nM; $K_i hA_1$, $K_i hA_{2A} > 10,000$) had the opposite effect on the affinity to hA_3AR . This could be possibly due to the additional steric hindrance caused by the phenylethyl group, which compromised the accommodation of relatively bulky bromo groups within the binding site and resulted in detrimental effects on hA_3AR affinities.

5.2. Molecular modeling studies

In order to rationalize the hA_3AR affinity profile observed for this new series of compounds, a receptor-driven molecular modeling investigation was carried out. All of the 2-(substituted)phenyl-pyrazolo[4,3-*e*]1,2,4-triazolo-[1,5-*c*]-pyrimidines were docked into the transmembrane (TM) binding cavity of the recently published hA_3AR model. Additionally, for the selected binding poses, individual electrostatic and hydrophobic contributions to the whole interaction energy of each receptor residue were calculated.

5.2.1. N^8 -Methyl derivatives

All of the N^8 -methyl-2-(substituted)phenyl-PTPs reported in this study (compounds **1–19**) showed affinities to hA_3AR in the nanomolar range. Compound **16** showed the highest affinity ($K_i hA_3 = 1.33$ nM). The hypothetical binding mode of this compound at hA_3AR is shown in Figure 1: ligand-recognition occurred in the upper region of the TM bundle, and the pyrazolo-triazolo-pyrimidine scaffold was surrounded by TMs 3, 5, 6 and 7 with the phenyl ring at the C^2 -position oriented towards TM2. Compound **16** was anchored by two stabilizing hydrogen-bonding interactions with the side chain of Asn250 (6.55) and an aromatic

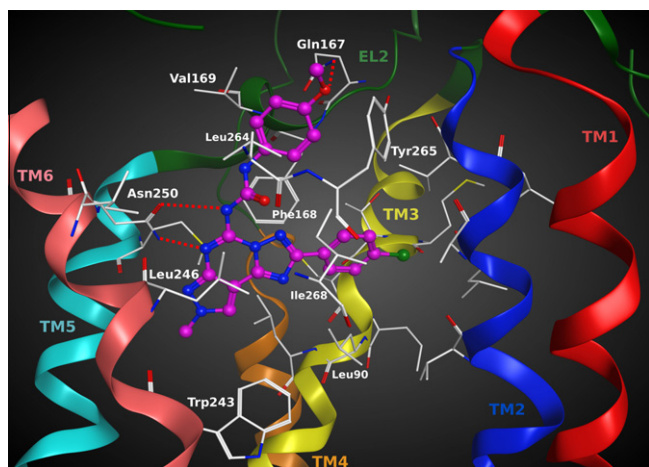


Figure 1. Hypothetical binding mode of the N^8 -methyl derivative **16** at the hA_3AR binding site obtained after docking simulation. Pose is viewed from the membrane side facing TM6, TM7 and TM1. The view of TM7 is voluntarily omitted. Side chains of some amino acids important for ligand recognition and H-bonding interactions are highlighted. Hydrogen atoms are not displayed.

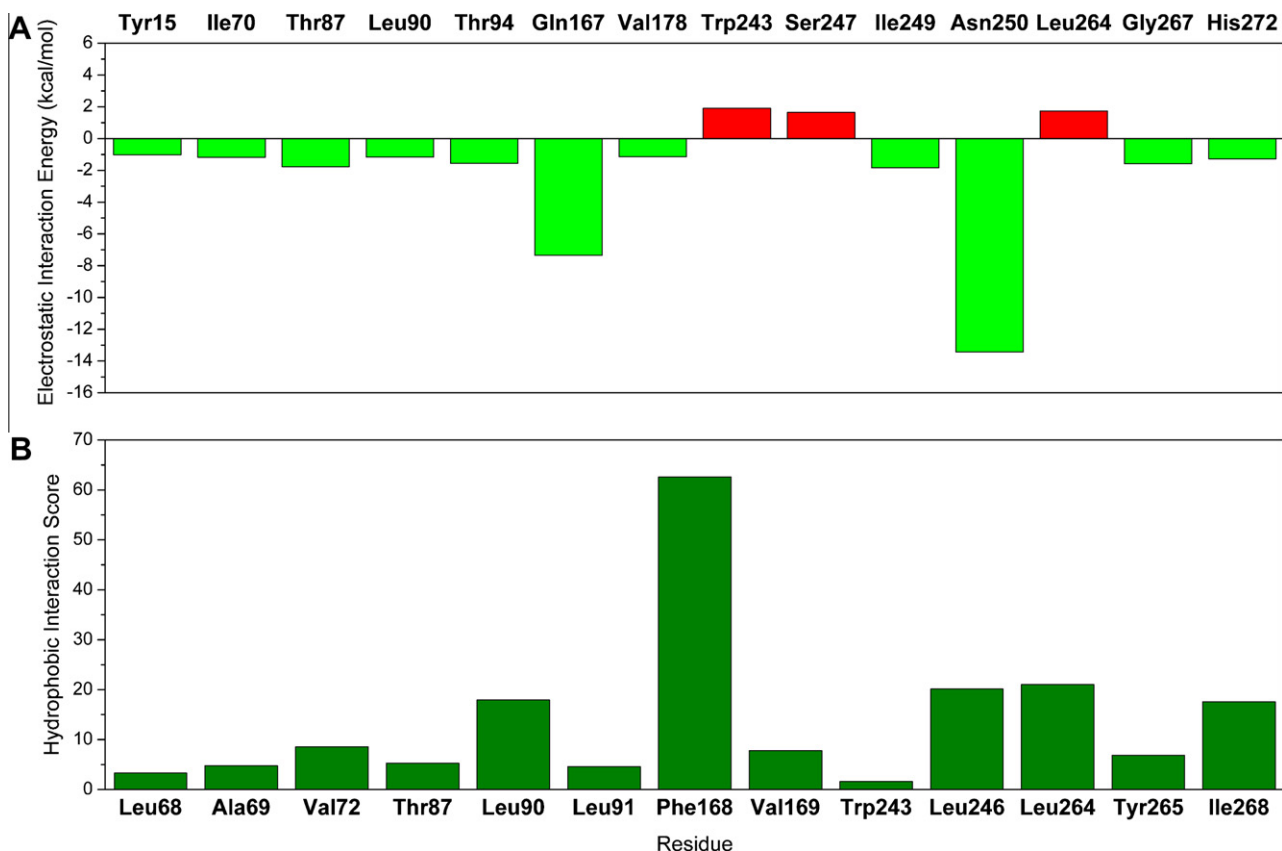


Figure 2. (A) Electrostatic interaction energy values (in kcal/mol) and (B) hydrophobic interaction scores (in arbitrary hydrophobic units) between the ligand and each single amino acid involved in ligand recognition calculated from the hypothetical binding mode of compound **16** inside the hA_3AR binding sites.

π - π stacking interaction with Phe168 (EL2). The asparagine residue 6.55, conserved among all AR subtypes, was already found to be important for ligand binding to hA₃AR.²⁷ Moreover, compound **16** formed hydrophobic interactions with many residues of the hA₃AR binding site including Leu91 (3.33), Phe168 (EL2), Leu246 (6.51), Ile268 (7.39) and the highly conserved Trp243 (6.48), an important residue in receptor activation and antagonist recognition²⁷; while the phenyl ring at the C²-position interacted with Val65 (2.57), Leu68 (2.60), Ala69 (2.61), Val72 (2.64), Thr87 (3.29), Leu90 (3.32); and the phenyl ring of the phenylcarbamoyl chain at N⁵ made hydrophobic contacts with Val169 (EL2), Leu264 (7.35) and Tyr265 (7.36). In addition, another H-bond was observed between the 4-methoxy group of the phenylcarbamoyl chain at N⁵ and the amide group of the side chain of Gln167 (EL2).

The observed interactions were confirmed by the analysis of the calculated electrostatic and hydrophobic contributions per residue to the whole interaction energy for the complex between hA₃AR and compound **16**. As shown in Figure 2, the main stabilizing contributions were associated with Asn250 (6.55) and Gln167 (EL2) (strong negative electrostatic interaction energy); while the strongest hydrophobic contributions were related to Phe168 (EL2), Leu264 (6.51), Leu246 (7.35), Leu90 (3.32) and Ile268 (7.39) (high hydrophobic interaction score). Overall, the hereby proposed binding mode of compound **16** to hA₃AR was very similar to the binding poses already described for previously reported PTP derivatives

and presented comparable interactions with the residues of the binding site.¹¹

Considering the N⁵-unsubstituted N⁸-methyl PTP derivatives, even if they showed binding modes to hA₃AR similar to the one observed for compound **16**, they lost some stabilizing hydrophobic interactions with Val169 (EL2), Leu264 (7.35) and Tyr265 (7.36) and this could explain the lower affinities to hA₃AR of the N⁵-unsubstituted derivatives as compared with the N⁵-substituted analogues. In addition, better hA₃AR selectivity profile against the other AR subtypes was also found in such N⁵-substituted derivatives. This could be attributed to the lack of space to accommodate bulky substituents at that position for the other AR subtypes. In particular, the weak binding of these compounds at hA_{2A}AR could be due to the different orientations that they acquired inside the hA_{2A} binding cleft as compared with the one observed inside hA₃AR. As already proposed for the previously reported PTP derivatives,¹¹ the presence of Glu169 (EL2) in hA_{2A}AR, which is mutated to Val169 (EL2) in hA₃AR, seemed to influence the binding poses of these compounds and led to the loss of good interactions with key residue Asn253 (6.55). Among the substituents at the N⁵-position, the phenylacetamide chain was more preferable than the phenylcarbamoyl chain for hA₃AR affinity, probably because of its higher flexibility that allowed better accommodation and stronger interaction in the binding cleft.

Regarding the effect of different *para*-substituents on the 2-phenyl ring towards affinity to hA₃AR, it appeared that the lateral cleft,

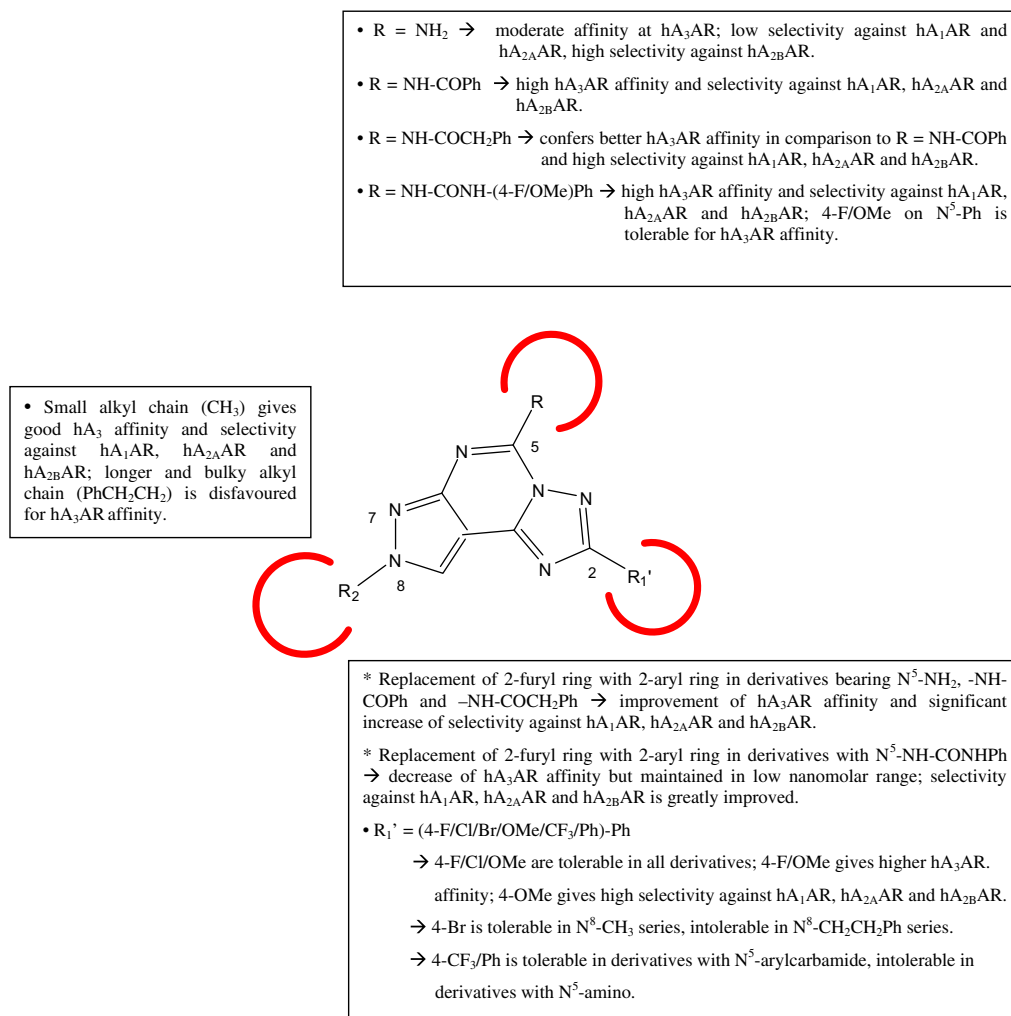


Figure 3. Structure–affinity relationship profile for the series of 2-(substituted)phenyl PTP derivatives **1–33**.

which accommodated the 2-phenyl ring, was not sufficiently spacious to host bulky substituents; this could account for the general decrease in hA₃AR affinity observed with the increase in molecular volume of the *para*-substituent on the 2-phenyl ring.

5.2.2. N⁸-Phenylethyl derivatives

The N⁸-phenylethyl derivatives hereby reported, in general, presented lower affinities to hA₃AR as compared with the N⁸-methyl analogues. Among them, the most affine derivative to this receptor was compound **30** (K_i hA₃ = 3.02 nM). The docking simulations on hA₃AR performed for this series of compounds showed a binding mode similar to the one observed for the N⁸-methyl derivatives, but with the PTP nucleus shifted up towards the entrance of the binding cavity. In fact, due to the presence of the bulkier N⁸-phenylethyl chain, these compounds bound less deeply into the binding site. As a consequence, these ligands were still able to form some interactions with the key residue Asn250 (6.55), but they were weaker than those observed for the N⁸-methyl derivatives. This finding seemed to explain the lower affinities of the N⁸-phenylethyl derivatives to hA₃AR as compared with the N⁸-methyl analogues.

For the substituents at both the N⁵-position of the PTP nucleus and the *para*-position of C²-phenyl ring, hypotheses similar to the ones reported above for the N⁸-methyl derivatives could be made. In fact, the introduction of a benzoyl or phenylacetyl group at the N⁵-position (compounds **25–33**) caused an increase in affinities to hA₃AR as compared with the N⁵-unsubstituted analogues (compounds **20–24**), mainly due to the increase in hydrophobic interactions with residues at the entrance of the hA₃AR binding site, such as Val169 (EL2), Ile253 (6.58), Val259 (EL3), Leu264 (7.35) and Tyr265 (7.36).

On the other hand, the presence of *para*-substituents on the 2-phenyl ring in these N⁸-phenylethyl derivatives was shown to be tolerable for binding to hA₃AR, provided they were not too bulky. As an illustration, the presence of a relatively bulky bromo group at the *para*-position in compound **33** was detrimental to hA₃AR affinity; this could probably be attributed to the additional steric hindrance caused by the phenylethyl group, which reduced the space to accommodate bulky substituents at the *para*-position of the 2-phenyl ring.

On the whole, the above-mentioned results have further defined the structure–affinity profiles of hA₃AR for the new 2-(substituted)phenyl-PTP scaffold (Fig. 3) and emphasized the importance of (i) a longer chain such as a benzamide or phenylacetamide group at the N⁵-position to confer higher affinity and better selectivity especially towards hA₁AR, hA_{2A}AR and hA_{2B}AR; (ii) a small methyl group at the N⁸-position in order to enhance both affinity and selectivity to the hA₃AR; (iii) a 2-(*para*-(un)substituted) phenyl ring at the C²-position to improve affinity and selectivity profiles to hA₃AR relative to their 2-furyl counterparts. Among the newly synthesized 2-(substituted)phenyl-PTP derivatives, compound **16**, with a 4-chlorophenyl at C², a small methyl group at N⁸ and a 4-methoxyphenylcarbamoyl chain at N⁵, showed the best hA₃AR affinity profile (K_i hA₃ = 1.33 nM) and good selectivities against the other ARs (hA₁/hA₃ = 4880; hA_{2A}/hA₃ = 1100).

6. Conclusions

Consistent with our previous findings, the bioisosteric replacement of the furan ring with a phenyl ring at the C²-position led to the identification of a new series of 2-(*para*-(un)substituted)phenyl-5-amide-8-substituted-pyrazolo-triazolo-pyrimidine derivatives with hA₃AR affinities and (or) selectivity profiles against the other AR subtypes better than those of the 2-furyl PTP derivatives. In addition, such substitution of 2-furyl

with an (un)substituted phenyl group could also potentially overcome the metabolic instability associated with the C²-furan ring. The present work has provided a complete structure–affinity relationship for 2-phenyl PTPs as potent and selective hA₃AR antagonists. Furthermore, the binding affinity profiles have also been successfully rationalized through molecular modeling investigations.

7. Experimental section

7.1. Chemistry

Reactions were routinely monitored by thin-layer chromatography (TLC) on silica gel plate (precoated 60 F₂₅₄ Merck plate). Column chromatographies were performed using Silica Gel 60 (Merck, 70–230 mesh). Melting points were determined on a Galenkamp instrument and were uncorrected. Compounds were dissolved in HPLC (high performance liquid chromatography)-grade methanol for determination of mass to charge ratio (m/z) via the LCQ Finnigan MAT mass spectrometer (source of ionization: atmospheric pressure chemical ionization (APCI) probe). Purity of compounds was detected by elemental analyses performed at the laboratory of microanalysis of the Department of Chemistry, University of Ferrara (Italy), and all the compounds were confirmed to achieve $\geq 95\%$ purity. ¹H spectra were determined in deuterated chloroform (CDCl₃) or deuterated dimethylsulfoxide (DMSO-*d*₆) through a Bruker DPX 300 spectrometer, with chemical shifts given in parts per million (δ) downfield relative to the central peak of the solvents, and *J* values (coupling constants) given in hertz. The following abbreviations were used: s, singlet; br s, broad singlet; d, doublet; dd, double doublet, br d, broad doublet; t, triplet; m, multiplet.

7.1.1. {(2*Z*)-2-Benzylidenehydrazino}methylene}malononitrile (A) and {(2*E*)-2 benzylidenehydrazino}methylene}malononitrile (B) (**4:1**) (**36**)

To solution of hydrazine hydrate (9.7 ml, 200 mmol) in absolute EtOH (350 ml) at 0 °C, benzaldehyde (21.2 ml, 200 mmol) was added. After 1.5 h, ethoxymethylenemalononitrile (24.4 g, 200 mmol) was added and the resulting solution was stirred for 1 h at room temperature. After cooling overnight, the yellowish precipitate was collected, washed with cold EtOH and recrystallized from CHCl₃.

Yield 82% ¹H NMR (300 MHz, DMSO-*d*₆): δ 7.43–7.52 (3H, m, aromatic H_{A+B}), 7.64–7.73 (2H, m, aromatic H_B), 7.76–7.84 (2H, m, aromatic H_A), 7.86 (1H, s, CH_A), 8.20 (1H, s, CH_A), 8.43 (1H, s, CH_B), 8.45 (1H, s, CH_B), 12.45 (1H, br s, NH_{A+B}).

7.1.2. {(2*Z*)-2-Benzylidene-1-methylhydrazino}methylene}malononitrile (**37**)

To solution of (19.6 g, 100 mmol) (2-benzylidenehydrazino)methylenemalononitrile in absolute EtOH (200 ml) and 1 M aqueous NaOH (110 mmol), methyl iodide (12.5 ml, 200 mmol) was added and the resulting solution was stirred at rt for 24 h. After cooling overnight, the yellowish product was filtered, washed with cold EtOH and recrystallized from EtOH.

The NMR characterization of intermediate **37** has been previously described in Ref. 18.

7.1.3. 4-Cyano-1-methylpyrazol-3-amine (**38**), 4-cyano-3-[(ethoxymethylene)amino]-1-methylpyrazole (**39**) and 5-amino-4-imino-2-methylpyrazolo[3,4-*d*]pyrimidine (**40**)

Both the preparation procedures and the NMR characterizations of intermediates **38**, **39** and **40** have been previously described in Refs. 12, 18 and 14, respectively.

7.1.4. General procedure for the preparation of 2-(substituted)-phenyl-8-methylpyrazolo[4,3-*e*][1,2,4]triazolo[1,5-*c*]pyrimidines (41–44)

The procedures for the preparation of intermediates 41–44 have been previously described in Ref. 14.

7.1.4.1. 2-(4-Chlorophenyl)-8-methylpyrazolo[4,3-*e*][1,2,4]triazolo[1,5-*c*]pyrimidine (41). Yield 45% ¹H NMR (300 MHz, DMSO-*d*₆): δ 4.21 (3H, s, Me), 7.64 (2H, d, *J* = 9 Hz, aromatic H), 8.23 (2H, d, *J* = 9 Hz, aromatic H), 8.92 (1H, s, pyrazolo-H), 9.46 (1H, s, pyrimidine-H).

7.1.4.2. 2-(4-Bromophenyl)-8-methylpyrazolo[4,3-*e*][1,2,4]triazolo[1,5-*c*]pyrimidine (42). Yield 64% ¹H NMR (300 MHz, DMSO-*d*₆): δ 4.21 (3H, s, Me), 7.78 (2H, d, *J* = 8 Hz, aromatic H), 8.16 (2H, d, *J* = 8 Hz, aromatic H), 8.92 (1H, s, pyrazolo-H), 9.46 (1H, s, pyrimidine-H).

7.1.4.3. 8-Methyl-2-(4-trifluoromethylphenyl)-pyrazolo[4,3-*e*][1,2,4]triazolo[1,5-*c*]pyrimidine (43). Yield 50% ¹H NMR (300 MHz, DMSO-*d*₆): δ 4.21 (3H, s, Me), 7.95 (2H, d, *J* = 8 Hz, aromatic H), 8.43 (2H, d, *J* = 8 Hz, aromatic H), 8.94 (1H, s, pyrazolo-H), 9.50 (1H, s, pyrimidine-H).

7.1.4.4. 2-(4-Biphenyl)-8-methylpyrazolo[4,3-*e*][1,2,4]triazolo[1,5-*c*]pyrimidine (44). Yield 50% ¹H NMR (300 MHz, DMSO-*d*₆): δ 4.21 (3H, s, Me), 7.42 (1H, t, *J* = 7 Hz, aromatic H), 7.52 (2H, t, *J* = 8 Hz, aromatic H), 7.78 (2H, d, *J* = 8 Hz, aromatic H), 7.89 (2H, d, *J* = 8 Hz, aromatic H), 8.32 (2H, d, *J* = 8 Hz, aromatic H), 8.93 (1H, s, pyrazolo-H), 9.48 (1H, s, pyrimidine-H).

7.1.5. General procedure for the preparation of 5(3)-[3-amino-2-methylpyrazol-4-yl]-3(5)-(phenyl)-1,2,4-triazoles (45–48)

A solution of the mixture of 41–44 (10 mmol) in 10% HCl (50 ml) was refluxed for 4–8 h depending on the substituent. Then the solution was cooled and basified with concentrated ammonium hydroxide. The resulting precipitate was filtered and washed with H₂O to afford the desired compounds 45–48 as solids.

7.1.5.1. 5(3)-[3-Amino-2-methylpyrazol-4-yl]-3(5)-(4-chlorophenyl)-[1,2,4]-1H-triazole (A:B 4.5:1) (45). Yield 87% ¹H NMR (300 MHz, DMSO-*d*₆): δ 3.69 (3H, s, Me_B), 3.71 (3H, s, Me_A), 5.27 (2H, s, NH₂/B), 5.53 (2H, s, NH₂/A), 7.52 (2H, d, *J* = 8 Hz, aromatic H_A), 7.63 (2H, d, *J* = 8 Hz, aromatic H_B), 7.87 (1H, s, pyrazolo-H_{A+B}), 8.08 (2H, d, *J* = 9 Hz, aromatic H_{A+B}), 13.88 (1H, s, NH_A), 14.30 (1H, s, NH_B).

7.1.5.2. 5(3)-[3-Amino-2-methylpyrazol-4-yl]-3(5)-(4-bromophenyl)-[1,2,4]-1H-triazole (A:B 4.1:1) (46). Yield 84% ¹H NMR (300 MHz, DMSO-*d*₆): δ 3.71 (3H, s, Me_{A+B}), 5.51 (2H, s, NH₂/A+B), 7.66 (2H, d, *J* = 8 Hz, aromatic H_A), 7.76 (2H, m, aromatic H_A), 7.88 (1H, s, pyrazolo-H_{A+B}), 8.02 (2H, d, *J* = 8 Hz, aromatic H_{A+B}), 13.90 (1H, s, NH_A) and 14.31 (1H, s, NH_B).

7.1.5.3. 5(3)-[3-Amino-2-methylpyrazol-4-yl]-3(5)-(4-trifluoromethylphenyl)-1,2,4-triazole (A:B 6.1:1) (47). Yield 88% ¹H NMR (300 MHz, DMSO-*d*₆): δ 3.67 (3H, s, Me_B), 3.71 (3H, s, Me_A), 5.26 (2H, s, NH₂/B), 5.54 (2H, s, NH₂/A), 7.83 (2H, d, *J* = 8 Hz, aromatic H_A), 7.89 (1H, s, pyrazolo-H_{A+B}), 7.94 (2H, d, *J* = 8 Hz, aromatic H_B), 8.24 (2H, d, *J* = 8 Hz, aromatic H_B), 8.27 (2H, d, *J* = 8 Hz, aromatic H_A), 14.00 (1H, s, NH_A), 14.50 (1H, s, NH_B).

7.1.5.4. 5(3)-[3-Amino-2-methylpyrazol-4-yl]-3(5)-(4-biphenyl)-1,2,4-triazole (A:B 2.5:1) (48). Yield 87% ¹H NMR (300 MHz, DMSO-*d*₆): δ 3.69 (3H, s, Me_B), 3.72 (3H, s, Me_A), 5.30 (2H, s, NH₂/B), 5.57 (2H, s, NH₂/A), 7.39 (1H, t, *J* = 7 Hz, aromatic H_{A+B}),

7.50 (2H, t, *J* = 7 Hz, aromatic H_{A+B}), 7.73 (2H, d, *J* = 8 Hz, aromatic H_A), 7.78 (2H, d, *J* = 8 Hz, aromatic H_{A+B}), 7.87 (2H, d, *J* = 8 Hz, aromatic H_{B-3'} and H_{B-5'}), 7.90 (1H, s, pyrazolo-H_{A+B}), 8.13 (2H, d, *J* = 8 Hz, aromatic H_B), 8.16 (2H, d, *J* = 8 Hz, aromatic H_A), 13.86 (1H, s, NH_A), 14.29 (1H, s, NH_B).

7.1.6. General procedure for the preparation of 2-(substituted)-phenyl-8-methyl-pyrazolo[4,3-*e*][1,2,4]triazolo[1,5-*c*]pyrimidin-5-amines (2–5)

To a solution of pyrazole derivatives 45–48 (10 mmol) in *N*-methylpyrrolidinone (40 ml), cyanamide (0.42 g, 60 mmol) and *p*-toluenesulfonic acid (2.85 g, 15 mmol) were added, and the mixture was heated at 160 °C for 4 h. Then cyanamide (0.42 g, 60 mmol) was added again and the solution was heated overnight. Then, the solution was diluted with hot water (100 ml) and triturated for 30 min and the precipitate (excess of cyanamide) was filtered off and washed with hot water (100 ml) again.

Compounds 2 and 3 have already been reported elsewhere.¹¹

7.1.6.1. 8-Methyl-2-(4-trifluoromethylphenyl)-pyrazolo[4,3-*e*][1,2,4]triazolo[1,5-*c*]pyrimidin-5-amine (4). Yield 63%, pale yellow solid, mp 299–300 °C (MeOH). ¹H NMR (300 MHz, DMSO-*d*₆): δ 4.04 (3H, s, Me), 7.70 (2H, s, NH₂), 7.95 (2H, d, aromatic H, *J* = 8 Hz), 8.43 (2H, d, aromatic H, *J* = 8 Hz), 8.61 (1H, s). MS-APCI (methanol) *m/z*: 334.2 (M+1)⁺. Anal. (C₁₄H₁₀N₇F₃) C, H, N.

7.1.6.2. 2-(4-Biphenyl)-8-methylpyrazolo[4,3-*e*][1,2,4]triazolo[1,5-*c*]pyrimidin-5-amine (5). Yield 85%, pale yellow solid, mp >300 °C (EtOH) ¹H NMR (300 MHz, DMSO-*d*₆): δ 4.04 (3H, s, Me), 7.42 (1H, t, *J* = 7 Hz), 7.52 (2H, t, *J* = 7 Hz), 7.65 (2H, s, NH₂), 7.78 (2H, d, *J* = 8 Hz), 7.88 (2H, d, *J* = 8 Hz), 8.32 (2H, d, *J* = 8 Hz), 8.61 (1H, s). MS-APCI (methanol) *m/z*: 342.4 (M+1)⁺. Anal. (C₁₉H₁₅N₇) C, H, N.

7.1.7. General procedure for the preparation of *N*-aryl-*N'*-(2-aryl-8-methyl-pyrazolo[4,3-*e*][1,2,4]triazolo[1,5-*c*]pyrimidin-5-yl)-ureas (8–19)

A mixture of amino compounds 2–5 (1 mmol) and the appropriate phenylisocyanate (4.5 mmol) in toluene (10 ml) was heated under reflux overnight. After cooling, the resulting mixture was filtered and washed with EtOH to afford the final compounds 8–19.

7.1.7.1. *N*-(2-(4-Chlorophenyl)-8-methylpyrazolo[4,3-*e*]-1,2,4-triazolo[1,5-*c*]pyrimidin-5-yl)-*N'*-phenylurea (8). Yield 72%, white solid, mp >300 °C (EtOH) ¹H NMR (300 MHz, DMSO-*d*₆): δ 4.15 (3H, s, Me), 7.13 (1H, t, aromatic H, *J* = 7 Hz), 7.41 (2H, t, aromatic H, *J* = 8 Hz), 7.60 (2H, d, aromatic H, *J* = 8 Hz), 7.67 (2H, d, aromatic H, *J* = 9 Hz), 8.32 (2H, d, aromatic H, *J* = 9 Hz), 8.82 (1H, s, pyrazolo H), 9.94 (1H, s, N'H), 10.94 (1H, s, NH). MS-APCI (methanol) *m/z*: 419.5 (M+1)⁺. Anal. (C₂₀H₁₅N₈OCl) C, H, N.

7.1.7.2. *N*-(2-(4-Bromophenyl)-8-methylpyrazolo[4,3-*e*]-1,2,4-triazolo[1,5-*c*]pyrimidin-5-yl)-*N'*-phenylurea (9). Yield 87%, white solid, mp >300 °C (EtOH) ¹H NMR (300 MHz, DMSO-*d*₆): δ 4.15 (3H, s, Me), 7.13 (1H, t, aromatic H, *J* = 8 Hz), 7.41 (2H, t, aromatic H, *J* = 8 Hz), 7.60 (2H, d, aromatic H, *J* = 8), 7.81 (2H, d, aromatic H, *J* = 8 Hz), 8.25 (2H, d, aromatic H, *J* = 8 Hz), 8.82 (1H, s, pyrazolo H), 9.95 (1H, s, N'H), 10.97 (1H, s, NH). MS-APCI (methanol) *m/z*: 464.3 (M+1)⁺. Anal. (C₂₀H₁₅N₈OBr) C, H, N.

7.1.7.3. *N*-(8-Methyl-2-(4-trifluoromethylphenyl)-pyrazolo[4,3-*e*]-1,2,4-triazolo[1,5-*c*]pyrimidin-5-yl)-*N'*-phenylurea (10). Yield 74%, white solid, mp 213–214 °C (EtOH) ¹H NMR (300 MHz, DMSO-*d*₆): δ 4.15 (3H, s, Me), 7.14 (1H, t, aromatic H, *J* = 7 Hz), 7.41 (2H, t, aromatic H, *J* = 8 Hz), 7.60 (2H, d, aromatic H, *J* = 8 Hz), 7.97 (2H, d, aromatic H, *J* = 8 Hz), 8.52 (2H, d, aromatic

H, $J = 8$ Hz), 8.84 (1H, s, pyrazolo H), 10.04 (1H, s, N'H), 10.97 (1H, s, NH). MS-APCI (methanol) m/z : 453.3 (M+1)⁺. Anal. (C₂₁H₁₅N₈OF₃) C, H, N.

7.1.7.4. *N*-(2-(4-Biphenyl)-8-methylpyrazolo[4,3-*e*]-1,2,4-triazolo[1,5-*c*]pyrimidin-5-yl)-*N'*-phenylurea (11). Yield 59%, pale brown solid, mp >300 °C (EtOH) ¹H NMR (300 MHz, DMSO-*d*₆): δ 4.16 (3H, s, Me), 7.14 (1H, t, aromatic H, $J = 7$ Hz), 7.37–7.47 (3H, m, aromatic H), 7.53 (2H, t, aromatic H, $J = 8$ Hz), 7.61 (2H, d, aromatic H, $J = 8$ Hz), 7.80 (2H, d, aromatic H, $J = 8$ Hz), 7.91 (2H, d, aromatic H, $J = 8$ Hz), 8.41 (2H, d, aromatic H, $J = 8$ Hz), 8.84 (1H, s, pyrazolo H), 9.93 (1H, s, N'H), 11.00 (1H, s, NH). MS-APCI (methanol) m/z : 460.4 (M+)⁺. Anal. (C₂₆H₂₀N₈O) C, H, N.

7.1.7.5. *N*-(2-(4-Chlorophenyl)-8-methylpyrazolo[4,3-*e*]-1,2,4-triazolo[1,5-*c*]pyrimidin-5-yl)-*N'*-(4-fluorophenyl)-urea (12). Yield 73%, white solid, mp >300 °C (EtOH) ¹H NMR (300 MHz, DMSO-*d*₆): δ 4.14 (3H, s, Me), 7.25 (2H, dd, aromatic H, $J = 9$ Hz, $J = 9$ Hz), 7.61 (2H, dd, aromatic H, $J = 9$ Hz, $J = 5$ Hz), 7.66 (2H, d, aromatic H, $J = 9$ Hz), 8.31 (2H, d, aromatic H, $J = 9$ Hz), 8.82 (1H, s, pyrazolo H), 9.97 (1H, s, N'H), 10.95 (1H, s, NH). MS-APCI (methanol) m/z : 437.6 (M+1)⁺. Anal. (C₂₀H₁₄N₈OFCl) C, H, N.

7.1.7.6. *N*-(2-(4-Bromophenyl)-8-methylpyrazolo[4,3-*e*]-1,2,4-triazolo[1,5-*c*]pyrimidin-5-yl)-*N'*-(4-fluorophenyl)-urea (13). Yield 72%, white solid, mp >300 °C (EtOH) ¹H NMR (300 MHz, DMSO-*d*₆): δ 4.14 (3H, s, Me), 7.25 (2H, dd, aromatic H, $J = 9$ Hz, $J = 9$ Hz), 7.61 (2H, dd, aromatic H, $J = 9$ Hz, $J = 5$ Hz), 7.80 (2H, d, aromatic H, $J = 8$ Hz), 8.24 (2H, d, aromatic H, $J = 8$ Hz), 8.82 (1H, s, pyrazolo H), 9.98 (1H, s, N'H), 10.94 (1H, s, NH). MS-APCI (methanol) m/z : 481.5 (M+)⁺. Anal. (C₂₀H₁₄N₈OBrF) C, H, N.

7.1.7.7. *N*-(4-Fluorophenyl)-*N'*-8-methyl-2-(4-trifluoromethylphenyl)-pyrazolo[4,3-*e*]-1,2,4-triazolo[1,5-*c*]pyrimidin-5-yl)-urea (14). Yield 74%, pale yellow solid, mp 298–299 °C (EtOH) ¹H NMR (300 MHz, DMSO-*d*₆): δ 4.14 (3H, s, Me), 7.24 (2H, dd, aromatic H, $J = 9$ Hz, $J = 9$ Hz), 7.60 (2H, dd, aromatic H, $J = 9$ Hz, $J = 5$ Hz), 7.95 (2H, d, aromatic H, $J = 8$ Hz), 8.49 (2H, d, aromatic H, $J = 8$ Hz), 8.81 (1H, s, pyrazolo H), 10.02 (1H, s, N'H), 10.94 (1H, s, NH). MS-APCI (methanol) m/z : 470.5 (M+)⁺. Anal. (C₂₁H₁₄N₈OF₄) C, H, N.

7.1.7.8. *N*-(2-(4-Biphenyl)-8-methylpyrazolo[4,3-*e*]-1,2,4-triazolo[1,5-*c*]pyrimidin-5-yl)-*N'*-(4-fluorophenyl)-urea (15). Yield 84%, white solid, mp >300 °C (EtOH) ¹H NMR (300 MHz, DMSO-*d*₆): δ 4.15 (3H, s, Me), 7.25 (2H, dd, aromatic H, $J = 9$ Hz, $J = 9$ Hz), 7.43 (1H, t, aromatic H, $J = 7$ Hz), 7.52 (2H, t, aromatic H, $J = 7$ Hz), 7.62 (2H, dd, aromatic H, $J = 9$ Hz, $J = 5$ Hz), 7.79 (2H, d, aromatic H, $J = 8$ Hz), 7.90 (2H, d, aromatic H, $J = 8$ Hz), 8.39 (2H, d, aromatic H, $J = 8$ Hz), 8.83 (1H, s, pyrazolo H), 9.94 (1H, s, N'H), 10.97 (1H, s, NH). MS-APCI (methanol) m/z : 479.5 (M+1)⁺. Anal. (C₂₆H₁₉N₈OF) C, H, N.

7.1.7.9. *N*-(2-(4-Chlorophenyl)-8-methylpyrazolo[4,3-*e*]-1,2,4-triazolo[1,5-*c*]pyrimidin-5-yl)-*N'*-(4-methoxyphenyl)-urea (16). Yield 94%, white solid, mp 252–253 °C (EtOH) ¹H NMR (300 MHz, DMSO-*d*₆): δ 3.77 (3H, s, OMe), 4.14 (3H, s, Me), 6.99 (2H, d, aromatic H, $J = 9$ Hz), 7.50 (2H, d, aromatic H, $J = 9$ Hz), 7.67 (2H, d, aromatic H, $J = 8$ Hz), 8.32 (2H, d, aromatic H, $J = 8$ Hz), 8.82 (1H, s, pyrazolo H), 9.85 (1H, s, N'H), 10.83 (1H, s, NH). MS-APCI (methanol) m/z : 448.4 (M+)⁺. Anal. (C₂₁H₁₇N₈O₂Cl) C, H, N.

7.1.7.10. *N*-(2-(4-Bromophenyl)-8-methylpyrazolo[4,3-*e*]-1,2,4-triazolo[1,5-*c*]pyrimidin-5-yl)-*N'*-(4-methoxyphenyl)-urea (17). Yield 84%, white solid, mp >300 °C (EtOH) ¹H NMR (300 MHz, DMSO-*d*₆): δ 3.77 (3H, s, OMe), 4.14 (3H, s, Me), 6.99 (2H, d, aromatic H, $J = 9$ Hz), 7.50 (2H, d, aromatic H, $J = 9$ Hz), 7.81 (2H, d, aromatic H, $J = 8$ Hz), 8.25 (2H, d, aromatic H, $J = 8$ Hz), 8.82 (1H, s, pyrazolo H), 9.85 (1H, s, N'H), 10.83 (1H, s, NH). MS-APCI (methanol) m/z : 494.2 (M+1)⁺. Anal. (C₂₁H₁₇N₈O₂Br) C, H, N.

7.1.7.11. *N*-(4-Methoxyphenyl)-*N'*-8-methyl-2-(4-trifluoromethylphenyl)-pyrazolo[4,3-*e*]-1,2,4-triazolo[1,5-*c*]pyrimidin-5-yl)-urea (18). Yield 59%, white solid, mp 211–213 °C (EtOH) ¹H NMR (300 MHz, DMSO-*d*₆): δ 3.77 (3H, s, OMe), 4.15 (3H, s, Me), 6.98 (2H, d, aromatic H, $J = 9$ Hz), 7.50 (2H, d, aromatic H, $J = 9$ Hz), 7.96 (2H, d, aromatic H, $J = 8$ Hz), 8.51 (2H, d, aromatic H, $J = 8$ Hz), 8.82 (1H, s, pyrazolo H), 9.91 (1H, s, N'H), 10.82 (1H, s, NH). MS-APCI (methanol) m/z : 483.2 (M+1)⁺. Anal. (C₂₂H₁₇N₈O₂F₃) C, H, N.

7.1.7.12. *N*-(2-(4-Biphenyl)-8-methylpyrazolo[4,3-*e*]-1,2,4-triazolo[1,5-*c*]pyrimidin-5-yl)-*N'*-(4-methoxyphenyl)-urea (19). Yield 55%, white solid, mp >300 °C (EtOH) ¹H NMR (300 MHz, DMSO-*d*₆): δ 3.77 (3H, s, OMe), 4.15 (3H, s, Me), 6.99 (2H, d, aromatic H, $J = 9$ Hz), 7.43 (1H, t, aromatic H, $J = 7$ Hz), 7.51 (2H, d, aromatic H, $J = 9$ Hz), 7.52 (2H, t, aromatic H, $J = 7$ Hz), 7.79 (2H, d, aromatic H, $J = 8$ Hz), 7.90 (2H, d, aromatic H, $J = 8$ Hz), 8.40 (2H, d, aromatic H, $J = 8$ Hz), 8.83 (1H, s, pyrazolo H), 9.81 (1H, s, N'H), 10.85 (1H, s, NH). MS-APCI (methanol) m/z : 490.2 (M+)⁺. Anal. (C₂₇H₂₂N₈O₂) C, H, N.

7.1.8. General procedure for the synthesis of *N*-(2-(substituted)-phenyl-8-phenylethyl-pyrazolo[4,3-*e*]-1,2,4-triazolo[1,5-*c*]pyrimidin-5-yl)benzamides (26, 27, 29)

To a suspension of 1 mmol of 2-(substituted)phenyl-8-phenylethylpyrazolo[4,3-*e*]-1,2,4-triazolo[1,5-*c*]pyrimidin-5-amine (21, 22, 24) in 10 mL of toluene, 1.81 g (8 mmol) of benzoic anhydride was added. The mixture was refluxed and stirred for 12 h at 120 °C. Then, the solvent was removed under reduced pressure and the residue was purified through column chromatography (AcOEt/petroleum ether in different ratios), to obtain the pure N⁵-substituted pyrazolo-triazolo-pyrimidine derivatives (26, 27 and 29).

7.1.8.1. *N*-[2-(4-Fluorophenyl)-8-phenylethyl-pyrazolo[4,3-*e*]-1,2,4-triazolo[1,5-*c*]pyrimidin-5-yl]benzamide (26). Yield 38%, pale yellow solid, mp 109–111 °C (AcOEt–petroleum ether) ¹H NMR (300 MHz, CDCl₃) δ: 3.34 (2H, t, Ph-CH₂, $J = 7$ Hz), 4.61 (2H, t, N⁸-CH₂, $J = 7$ Hz), 7.07 (2H, d, aromatic H, $J = 6$ Hz), 7.12–7.24 (5H, m, aromatic H), 7.54–7.71 (3H, m, aromatic H), 7.95 (1H, s, pyrazolo-H), 8.07 (2H, d, aromatic H, $J = 7$ Hz), 8.27 (2H, dd, aromatic H, $J = 6$ Hz, $J = 6$ Hz), 9.81 (1H, s, NH). MS-APCI (methanol) m/z : 478.8 (M+1)⁺ Anal. (C₂₇H₂₀N₇OF) C, H, N.

7.1.8.2. *N*-[2-(4-Chlorophenyl)-8-phenylethyl-pyrazolo[4,3-*e*]-1,2,4-triazolo[1,5-*c*]pyrimidin-5-yl]benzamide (27). Yield 50%, pale yellow solid, mp 112–114 °C (AcOEt–petroleum ether) ¹H NMR (300 MHz, CDCl₃) δ: 3.33 (2H, t, Ph-CH₂, $J = 7$ Hz), 4.61 (2H, t, N⁸-CH₂, $J = 7$ Hz), 7.07 (2H, d, aromatic H, $J = 6$ Hz), 7.21–7.24 (3H, m, aromatic H), 7.49 (2H, d, aromatic H, $J = 8$ Hz), 7.58–7.68 (3H, m, aromatic H), 7.95 (1H, s, pyrazolo-H), 8.07 (2H, d, aromatic H, $J = 7$ Hz), 8.27 (2H, d, aromatic H, $J = 8$ Hz), 9.80 (1H, s, NH). MS-APCI (methanol) m/z : 494.9 (M+)⁺ Anal. (C₂₇H₂₀N₇OCl) C, H, N.

7.1.8.3. *N*-[2-(4-Methoxyphenyl)-8-phenylethyl-pyrazolo[4,3-*e*]-1,2,4-triazolo[1,5-*c*]pyrimidin-5-yl]benzamide (29). Yield 22%, pale yellow solid, mp 113–115 °C (AcOEt–petroleum ether) ¹H NMR (300 MHz, CDCl₃) δ: 3.34 (2H, t, Ph-CH₂, *J* = 7 Hz), 3.89 (3H, s, OCH₃), 4.61 (2H, t, N⁸-CH₂, *J* = 7 Hz), 7.03 (2H, d aromatic H, *J* = 9 Hz), 7.07 (2H, d, aromatic H, *J* = 7 Hz), 7.22–7.24 (3H, m, aromatic H), 7.58–7.68 (3H, m, aromatic H), 7.95 (1H, s, pyrazolo-H), 8.07 (2H, d, aromatic H, *J* = 8 Hz), 8.21 (2H, d, aromatic H, *J* = 8 Hz), 9.84 (1H, s, NH) MS-APCI (methanol) *m/z*: 491.2 (M+2)⁺ Anal. (C₂₈H₂₃N₇O₂) C, H, N.

7.1.9. General procedure for the synthesis of *N*-(2-(substituted)-phenyl-8-phenylethyl-pyrazolo[4,3-*e*]-1,2,4-triazolo[1,5-*c*]pyrimidin-5-yl)phenylacetamides (30–33)

To a suspension of 1 mmol of 2-(substituted)phenyl-8-phenylethyl-pyrazolo[4,3-*e*]-1,2,4-triazolo[1,5-*c*]pyrimidin-5-amine (20–23) in 10 mL of toluene, 1.1 mL (8 mmol) of phenylacetyl chloride was added, followed by 1.4 mL (8 mmol) of DIPEA. The mixture was refluxed and stirred for 24 h at 120 °C. Then, the solvent was removed under reduced pressure and the residue was purified via column chromatography (AcOEt: Petroleum Ether in different ratios), to obtain the pure N⁵-substituted pyrazolo-triazolo-pyrimidine derivatives (30–33).

7.1.9.1. *N*-[2-(Phenyl)-8-phenylethyl-pyrazolo[4,3-*e*]-1,2,4-triazolo[1,5-*c*]pyrimidin-5-yl]phenylacetamide (30). Yield 19%, yellow solid, mp 92–94 °C (AcOEt–petroleum ether) ¹H NMR (300 MHz, CDCl₃) δ: 3.34 (2H, t, Ph-CH₂, *J* = 7 Hz), 4.51 (2H, s, CH₂-CO), 4.61 (2H, t, N⁸-CH₂, *J* = 7 Hz), 7.07 (2H, d, aromatic H, *J* = 6 Hz), 7.18–7.23 (3H, m, aromatic H), 7.32–7.43 (5H, m, aromatic H), 7.49–7.51 (3H, m, aromatic H), 7.95 (1H, s, pyrazolo-H), 8.16–8.20 (2H, br d, aromatic H), 9.18 (1H, s, NH). MS-APCI (methanol) *m/z*: 475.2 (M+2)⁺. Anal. (C₂₈H₂₃N₇O) C, H, N.

7.1.9.2. *N*-[2-(4-Fluorophenyl)-8-phenylethyl-pyrazolo[4,3-*e*]-1,2,4-triazolo[1,5-*c*]pyrimidin-5-yl]phenylacetamide (31). Yield 26%, yellow solid, mp 107–109 °C (AcOEt–petroleum ether) ¹H NMR (300 MHz, CDCl₃) δ: 3.33 (2H, t, Ph-CH₂, *J* = 7 Hz), 4.50 (2H, s, CH₂-CO), 4.60 (2H, t, N⁸-CH₂, *J* = 7 Hz), 7.07 (2H, d, aromatic H, *J* = 6 Hz), 7.15–7.23 (5H, m, aromatic H), 7.32–7.43 (5H, m, aromatic H), 7.94 (1H, s, pyrazolo-H), 8.17 (2H, dd, aromatic H, *J* = 6 Hz, *J* = 6 Hz), 9.14 (1H, s, NH). MS-APCI (methanol) *m/z*: 492.6 (M+1)⁺. Anal. (C₂₈H₂₂N₇OF) C, H, N.

7.1.9.3. *N*-[2-(4-Chlorophenyl)-8-phenylethyl-pyrazolo[4,3-*e*]-1,2,4-triazolo[1,5-*c*]pyrimidin-5-yl]phenylacetamide (32). Yield 20%, yellow solid, mp 108–110 °C (AcOEt–petroleum ether) ¹H NMR (300 MHz, CDCl₃) δ: 3.33 (2H, t, Ph-CH₂, *J* = 7 Hz), 4.49 (2H, s, CH₂-CO), 4.61 (2H, t, N⁸-CH₂, *J* = 7 Hz), 7.07 (2H, d, aromatic H, *J* = 7 Hz), 7.17–7.23 (3H, m, aromatic H), 7.33–7.43 (5H, m, aromatic H), 7.47 (2H, d, aromatic H, *J* = 8 Hz), 7.93 (1H, s, pyrazolo-H), 8.11 (2H, d, aromatic H, *J* = 8 Hz), 9.14 (1H, s, NH). MS-APCI (methanol) *m/z*: 508.6 (M+)⁺. Anal. (C₂₈H₂₂N₇OCl) C, H, N.

7.1.9.4. *N*-[2-(4-Bromophenyl)-8-phenylethyl-pyrazolo[4,3-*e*]-1,2,4-triazolo[1,5-*c*]pyrimidin-5-yl]phenylacetamide (33). Yield 24%, yellow solid, mp 279–281 °C (AcOEt–petroleum ether) ¹H NMR (300 MHz, CDCl₃) δ: 3.34 (2H, t, Ph-CH₂, *J* = 7 Hz), 4.50 (2H, s, CH₂-CO), 4.61 (2H, t, N⁸-CH₂, *J* = 7 Hz), 7.07 (2H, d, aromatic H, *J* = 8 Hz), 7.19–7.23 (3H, m, aromatic H), 7.33–7.45 (5H, m, aromatic H), 7.64 (2H, d, aromatic H, *J* = 8 Hz), 7.93 (1H, s, pyrazolo-H), 8.05 (2H, d, aromatic H, *J* = 8 Hz), 9.13 (1H, s, NH). MS-APCI (methanol) *m/z*: 552.5 (M+)⁺. Anal. (C₂₈H₂₂N₇OBr) C, H, N.

7.2. Biology

7.2.1. CHO membrane preparation

All the pharmacological methods involved in membrane preparation for radioligand binding experiments and adenylyl cyclase activity assays followed the procedures as described earlier.¹⁹

Membranes for radioligand binding were prepared from cells stably transfected with the human adenosine receptor subtypes (hA₁AR, hA_{2A}AR, and hA₃AR expressed on CHO cells) in a two-step procedure. In the first low-speed step (1000g for 4 min), the cell fragments and nuclei were removed. After that, the crude membrane fraction was sedimented from the supernatant at 100,000g for 30 min. The membrane pellet was then resuspended in the specific buffer used for the respective binding experiments, frozen in liquid nitrogen and stored at –80 °C. For the measurement of the adenylyl cyclase activity in hA_{2B}AR expressed on CHO cells, only one step of centrifugation was used, in which the homogenate was sedimented for 30 min at 54,000g. The resulting crude membrane pellet was resuspended in 50 mM Tris/HCl, pH 7.4 and immediately used for the adenylyl cyclase assay.

7.2.2. Human cloned A₁, A_{2A}, A₃ AR binding assay

Binding of [³H]-CCPA to CHO cells transfected with the human recombinant A₁AR was performed as previously described.^{19,20} Displacement experiments were performed for 3 h at 25 °C in 200 μL of buffer containing 1 nM [³H] CCPA, 0.2 U/mL adenosine deaminase, 20 μg of membrane protein in 50 mM Tris/HCl, pH 7.4 and tested compound in different concentrations. Nonspecific binding was determined in the presence of 1 mM theophylline.²¹

Binding of 30 nM [³H]-NECA to CHO cells transfected with the human recombinant A_{2A}ARs was performed following the conditions as that described for the hA₁AR binding assay.^{19,20} In the displacement experiments, sample with 50 μg of membrane protein in 50 mM Tris/HCl, 10 mM MgCl₂, pH 7.4 and tested compound in different concentrations was incubated for 3 h at 25 °C. Nonspecific binding was determined in the presence of 100 μM R-PIA (R-N⁶-phenylisopropyladenosine).²¹

Binding of [³H]-NECA to CHO cells transfected with the human recombinant A₃ARs was carried out as previously described.^{19,20} The displacement experiments were performed for 3 h at 25 °C in buffer solution containing 10 nM [³H]-NECA, 20 μg of membrane protein in 50 mM Tris/HCl, 1 mM EDTA (ethylenediaminetetraacetate), 10 mM MgCl₂, pH 8.25 and tested compound in different concentrations. Nonspecific binding was determined in the presence of 100 μM R-PIA.²¹

Bound and free radioactivity was separated by filtering the assay mixture through Whatman GF/B glass-fiber filters using a Micro-Mate 196-cell harvester (Packard Instrument Company). The filter bound radioactivity was counted on Top Count (efficiency of 57%) with Micro-Scint 20. The protein concentration was determined according to the Bio-Rad method²⁸ with bovine albumin used as a reference standard.

7.2.3. Adenylyl cyclase activity

Due to the lack of a suitable radioligand for hA_{2B}AR in binding assay, the potency of antagonists at hA_{2B}AR (expressed on CHO cells) was determined in adenylyl cyclase experiments instead. The procedure was carried out as described previously with minor modifications.^{19,20} Membranes were incubated with about 150,000 cpm of [^α-³²P]ATP for 20 min in the incubation mixture as described^{19,20} without EGTA and NaCl. The IC₅₀ values of tested antagonists for concentration-dependent inhibition of NECA-stimulated adenylyl cyclase were calculated accordingly. Dissociation constants (K_i) of the antagonists were then calculated from the Cheng and Prusoff equation.²²

7.3. Molecular modeling

7.3.1. General

All the modeling studies were carried out on a 20 CPU (Intel Core2 Quad CPU 2.40 GHz) Linux cluster. Homology modeling, energy calculation, and analyses of docking poses were performed using the Molecular Operating Environment (MOE, version 2010.10) suite.²⁹ The software package MOPAC,³⁰ implemented in MOE suite, was utilized for all quantum mechanical calculations. Docking simulations were performed using GOLD suite 5.0.1.³¹

7.3.2. Homology model of hA₃AR

Based on the assumption that GPCRs share similar TM boundaries and overall topology, a homology model of the hA₃AR was constructed as previously reported,^{23,24} based on a template of the crystallographic structure of hA_{2A}AR in complex with the antagonist ZM-241385 (PDB code: 3EML).²⁵ The numbering of the amino acids follows the arbitrary scheme by Ballesteros and Weinstein. According to this scheme, each amino acid identifier starts with the helix number, followed by the position relative to a reference residue among the most conserved amino acid in that helix. The number 50 is arbitrarily assigned to the reference residue.³²

Firstly, the amino acid sequences of TM helices of the hA₃AR were aligned with those of the template, guided by the highly conserved amino acid residues, including the DRY motif (Asp3.49, Arg3.50, and Tyr3.51) and three proline residues (Pro4.60, Pro6.50, and Pro7.50) in the TM segments of GPCRs. The same boundaries were applied for the TM helices of hA₃AR as they were identified from the 3D structure of the template, the coordinates of which were used to construct the seven TM helices for hA₃AR. Then, the loop domains were constructed by the loop search method implemented in MOE on the basis of the structure of compatible fragments found in Protein Data Bank. In particular, loops were modeled first in random order. For each loop, a contact energy function analyzed the list of candidates collected in the segment searching stage, taking into account all atoms already modeled and any atoms specified by the user as belonging to the model environment. These energies were then used to make a Boltzmann-weighted choice from the candidates, the coordinates of which were then copied to the model. Subsequently, the side chains were modeled using a library of rotamers generated by systematic clustering of the Protein Data Bank data via the same procedure. Side chains of residues whose backbone coordinates were copied from a template were modeled first, followed by side chains of modeled loops. Gaps and their side chains were modeled last.

Special caution has to be given to the second extracellular loop (EL2) because amino acids of this loop could be involved in direct interactions with the ligands. A driving force to the peculiar fold of EL2 might be the presence of a disulfide bridge between cysteines in TM3 and EL2. Since this covalent link is conserved in both hA_{2A}AR and hA₃AR, the EL2 loop was modeled using a constrained geometry around the EL2–TM3 disulfide bridge. The constraints were applied before the construction of the homology model, especially during the sequences alignment, by selecting the cysteine residues involved in the disulfide bridge of hA_{2A}AR to be constrained with the corresponding cysteine residues in hA₃AR sequence. In particular, Cys166 (EL2) and Cys77 (3.25) of the hA_{2A}AR were constrained with Cys166 (EL2) and Cys83 (3.25) of the hA₃AR, respectively. During the alignment, MOE-Align attempted to minimize the number of constraint violations. At the end of the homology modeling, the presence of the conserved disulfide bridge in the model was manually checked.

After the heavy atoms were modeled, all hydrogen atoms were added using the Protonate 3D methodology,³³ part of the MOE suite. This application assigned a protonation state to each chemi-

cal group that minimized the total free energy of the system (taking titration into account).³³ Protein stereochemistry evaluation was then performed by several tools (Ramachandran plot; backbone bond lengths, angles and dihedral plots; clash contacts report; rotamers strain energy report) implemented in MOE suite.²⁹

7.3.3. Molecular docking of hA₃AR antagonists

Ligand structures were built using MOE-builder tool, part of the MOE suite,²⁹ and were subjected to MMFF94x energy minimization until the rms of conjugate gradient was <0.05 kcal mol⁻¹ Å⁻¹. Partial charges for the ligands were calculated using PM3/ESP methodology. Four different programs have been used to calibrate our docking protocol: MOE-Dock,²⁹ GOLD,³¹ Glide,³⁴ and PLANTS.³⁵ In particular, ZM-241385 was re-docked into the crystal structure of the hA_{2A}AR (PDB code: 3EML) with different docking algorithms and scoring functions, as already described.^{23,24} Then, RMSD values between predicted and crystallographic poses of ZM-241385 were calculated for each of the docking algorithms. The results showed that docking simulations performed with Gold gave the lowest RMSD value, the lowest mean RMSD value and the highest number of poses with RMSD value <2.5 Å.

On the basis of the best docking performance, all antagonist structures were docked into the hypothetical TM binding site of the hA₃AR model using the docking tool of the GOLD suite.³² Searching was conducted within a user-specified docking sphere using the Genetic Algorithm protocol and the GoldScore scoring function. GOLD performs a user-specified number of independent docking runs (25 in our specific case) and writes the resulting conformations and their energies in a molecular database file. The resulting docked complexes were subjected to MMFF94x energy minimization until the rms of conjugate gradient was <0.1 kcal mol⁻¹ Å⁻¹. Charges for the ligands were imported from the MOPAC output files using PM3/ESP methodology.

Prediction of antagonist-receptor complex stability (in terms of corresponding pK_i value) and the quantitative analysis of non-bonded intermolecular interactions (H-bonds, transition metal, water bridges, hydrophobic, electrostatic) were calculated and visualized using several tools implemented in MOE suite.²⁹ Electrostatic and hydrophobic contributions to the binding energy of individual amino acids have been calculated as implemented in MOE suite.²⁹ In order to estimate the electrostatic contributions, atomic charges for the ligands were calculated using PM3/ESP methodology. Partial charges for protein amino acids were calculated on the basis of the AMBER99 force field.

Acknowledgments

This work has been supported by the National University of Singapore (FRC grant, R-148-000-129-112), Ministry of Education (MOE2009-T2-2-011 project, R-398-000-068-112) and A-STAR (TSRP project, R-148-001-435-305). The molecular modeling work coordinated by S.M. has been carried out with financial support from the University of Padova, Italy, and the Italian Ministry for University and Research, Rome, Italy (MIUR, PRIN2008: protocol number 200834TC4L_002). S.M. is also very grateful to Chemical Computing Group for the scientific and technical partnership.

Supplementary data

Supplementary data associated with this article can be found, in the online version, at doi:10.1016/j.bmc.2011.08.026.

References and notes

1. Jacobson, K. A.; Gao, Z. G. *Nat. Rev. Drug Disc.* **2006**, *5*, 247.
2. Moro, S.; Gao, Z. G.; Jacobson, K. A.; Spalluto, G. *Med. Res. Rev.* **2006**, *26*, 131.

3. Jacobson, K. A. *Trends Pharmacol. Sci.* **1998**, *19*, 184.
4. Merighi, S.; Mirandola, P.; Varani, K.; Gessi, S.; Leung, E.; Baraldi, P. G.; Tabrizi, M. A.; Borea, P. A. *Pharmacol. Ther.* **2003**, *100*, 31.
5. Müller, C. E.; Jacobson, K. A. *Biochim. Biophys. Acta* **2011**, *1808*, 1290.
6. Fredholm, B. B.; IJzerman, A. P.; Jacobson, K. A.; Linden, J.; Müller, C. E. *Pharmacol. Rev.* **2011**, *63*, 1.
7. Baraldi, P. G.; Cacciari, B.; Borea, P. A.; Varani, K.; Pastorin, G.; Da Ros, T.; Tabrizi, M. A.; Fruttarolo, F.; Spalluto, G. *Curr. Pharm. Des.* **2002**, *8*, 2299.
8. Baraldi, P. G.; Cacciari, B.; Romagnoli, R.; Klotz, K. N.; Spalluto, G.; Varani, K.; Gessi, S.; Merighi, S.; Borea, P. A. *Drug Dev. Res.* **2001**, *53*, 225.
9. Maconi, A.; Pastorin, G.; Da Ros, T.; Spalluto, G.; Gao, Z. G.; Jacobson, K. A.; Baraldi, P. G.; Cacciari, B.; Varani, K.; Borea, P. A. *J. Med. Chem.* **2002**, *45*, 3579.
10. Baraldi, P. G.; Cacciari, B.; Moro, S.; Spalluto, G.; Pastorin, G.; Da Ros, T.; Klotz, K.-N.; Varani, K.; Gessi, S.; Borea, P. A. *J. Med. Chem.* **2002**, *45*, 770.
11. Cheong, S. L.; Dolzhenko, A.; Kachler, S.; Paoletta, S.; Federico, S.; Cacciari, B.; Dolzhenko, A.; Klotz, K. N.; Moro, S.; Spalluto, G.; Pastorin, G. *J. Med. Chem.* **2010**, *53*, 3361.
12. Gatta, F.; Del Giudice, M. R.; Borioni, A.; Borea, P. A.; Dionisotti, S.; Ongini, E. *Eur. J. Med. Chem.* **1993**, *28*, 569.
13. Schmidt, P.; Eichenberger, K.; Wilhelm, M.; Druey, J. *Helv. Chim. Acta* **1959**, *42*, 763.
14. Dolzhenko, A. V.; Pastorin, G.; Dolzhenko, A. V.; Chui, W. K. *Tetrahedron Lett.* **2009**, *50*, 5617.
15. Baraldi, P. G.; Cacciari, B.; Spalluto, G.; Ji, X.-D.; Olah, M. E.; Stiles, G.; Dionisotti, S.; Zocchi, C.; Ongini, E.; Jacobson, K. A. *J. Med. Chem.* **1996**, *39*, 802.
16. Baraldi, P. G.; Cacciari, B.; Pineda de Las Infantas, M. J.; Romagnoli, R.; Spalluto, G.; Volpini, R.; Costanzi, S.; Vittori, S.; Cristalli, G.; Melman, N.; Park, K.-S.; Ji, X.-D.; Jacobson, K. A. *J. Med. Chem.* **1998**, *41*, 3174.
17. Baraldi, P. G.; Cacciari, B.; Romagnoli, R.; Spalluto, G.; Moro, S.; Klotz, K. N.; Leung, E.; Varani, K.; Gessi, S.; Merighi, S.; Borea, P. A. *J. Med. Chem.* **2000**, *43*, 4768.
18. Baraldi, P. G.; Bovero, A.; Fruttarolo, F.; Romagnoli, R.; Tabrizi, M. A.; Pretia, D.; Varani, K.; Borea, P. A.; Moorman, A. R. *Bioorg. Med. Chem.* **2003**, *11*, 4161.
19. Klotz, K. N.; Hessling, J.; Hegler, J.; Owman, C.; Kull, B.; Fredholm, B. B.; Lohse, M. J. *Naunyn-Schmiedeberg's Arch. Pharmacol.* **1998**, *357*, 1.
20. Klotz, K. N.; Cristalli, G.; Grifantini, M.; Vittori, S.; Lohse, M. J. *J. Biol. Chem.* **1985**, *260*, 14659.
21. De Lean, A.; Hancock, A. A.; Lefkowitz, R. J. *Mol. Pharmacol.* **1982**, *21*, 5.
22. Cheng, Y. C.; Prusoff, H. R. *Biochem. Pharmacol.* **1973**, *22*, 3099.
23. Lenzi, O.; Colotta, V.; Catarzi, D.; Varano, F.; Poli, D.; Filacchioni, G.; Varani, K.; Vincenzi, F.; Borea, P. A.; Paoletta, S.; Morizzo, E.; Moro, S. *J. Med. Chem.* **2009**, *52*, 7640.
24. Morizzo, E.; Federico, S.; Spalluto, G.; Moro, S. *Curr. Pharm. Des.* **2009**, *15*, 4069.
25. Jaakola, V. P.; Griffith, M. T.; Hanson, M. A.; Cherezov, V.; Chien, E. Y. T.; Lane, J. R.; IJzerman, A. P. *Science* **2008**, *322*, 1211.
26. Pastorin, G.; Da Ros, T.; Spalluto, G.; Deflorian, F.; Moro, S.; Cacciari, B.; Baraldi, P. G.; Gessi, S.; Varani, K.; Borea, P. A. *J. Med. Chem.* **2003**, *46*, 4287.
27. Gao, Z. G.; Chen, A.; Barak, D.; Kim, S.-K.; Muller, C. E.; Jacobson, K. A. *J. Biol. Chem.* **2002**, *277*, 19056.
28. Bradford, M. M. *Anal. Biochem.* **1976**, *72*, 248.
29. MOE (Molecular Operating Environment), version 2010.10; software available from Chemical Computing Group Inc. (1010 Sherbrooke Street West, Suite 910, Montreal, Quebec, Canada H3A 2R7); <http://www.chemcomp.com>.
30. Stewart, J. J. P. MOPAC 7; Fujitsu Limited: Tokyo, Japan, 1993.
31. GOLD suite, version 5.0.1; software available from Cambridge Crystallographic Data Centre Cambridge Crystallographic Data Centre (12 Union Road Cambridge CB2 1EZ UK); <http://www.ccdc.cam.ac.uk>.
32. Ballesteros, J. A.; Weinstein, H. *Methods Neurosci.* **1995**, *25*, 366.
33. Labute, P. *Proteins* **2009**, *75*, 187.
34. Halgren, T. A.; Murphy, R. B.; Friesner, R. A.; Beard, H. S.; Frye, L. L.; Pollard, W. T.; Banks, J. L. *J. Med. Chem.* **2004**, *47*, 1750.
35. Korb, O.; Stützle, T.; Exner, T. E. *J. Chem. Inf. Model.* **2009**, *49*, 84.